2016•2017
FACULTY OF MEDICINE AND LIFE SCIENCES
Master of Biomedical Sciences

Master's thesis

The use of a specific HDAC3 inhibitor to modulate macrophage polarization in order to improve functional recovery after spinal cord injury

Supervisor :
Prof. dr. Sven HENDRIX

Paulien Baeten

Thesis presented in fulfillment of the requirements for the degree of Master of Biomedical Sciences

Transnational University Limburg is a unique collaboration of two universities in two countries: the University of Hasselt and Maastricht University.

universiteit hasselt
KNOWLEDGE IN ACTION

Universiteit Hasselt | Campus Hasselt | Martelarenlaan 42 | BE-3500 Hasselt
Universiteit Hasselt | Campus Diepenbeek | Agoralaan Gebouw D | BE-3590 Diepenbeek

universiteit hasselt | Maastricht University

2016•2017
FACULTY OF MEDICINE AND LIFE SCIENCES
Master of Biomedical Sciences

Master's thesis

The use of a specific HDAC3 inhibitor to modulate macrophage polarization in order to improve functional recovery after spinal cord injury

Supervisor :
Prof. dr. Sven HENDRIX

Paulien Baeten
Thesis presented in fulfillment of the requirements for the degree of Master of Biomedical Sciences

universiteit hasselt | Maastricht University

PREFACE

This senior internship offered by Hasselt University in collaboration with Maastricht University, gave me the opportunity to learn many new skills. I gained a lot of experience on working in the lab, planning experiments, communicating results and how to think outside of the box. I believe this internship allowed me to be fully prepared for my future career as a biomedical scientist.

I am very thankful I could do this internship in the group of morphology of Prof. dr. Sven Hendrix at BIOMED, Hasselt University. This research group has a lot of experience in both *in vitro* and *in vivo* experiments. I am grateful everyone was willing to pass all this information on to me. I am sure I will be able to use all these achieved skills in the future. In particular, I want to thank Selien Sanchez for her support, patience and trust in me. She was a very good, enthusiastic and stimulating supervisor inside and outside the lab. I wish her the best of luck with her future experiments in her doctoral research! To the other team members Stefanie Lemmens, Daniela Sommer, Leen Timmermans and Céline Erens: thanks for the warm welcome and for all your help and good luck! Lastly, I would like to thank Prof. Hendrix for stimulating my scientific mind and providing me with useful input and scientific challenges. Altogether, they form a very tight group with expertise, friendship and fun and they are always there to help each other out.

Together with my fellow-students at BIOMED, I survived this stressful but educative period. It was interesting to follow how everyone progressed with their research and successfully finalized it. They were always ready for a chat, some tips or to help one another out. I will miss our weekly lunch meetings on Friday and the fun in our cosy office! Good luck to all of you!

I would like to thank my family for all their support. Although it were difficult times, they managed to stimulate and encourage me throughout my internship. In addition, thanks to my friends who were always there for me to take my mind of the work and worries and especially to the ones who were truly interested in my research. Another person who is very important to me is Daan. He patiently listened and said the right words to help me out or keep my feet on the ground, so thanks for being there for me!

Despite the sacrifices I made to successfully complete this thesis, I believe my life will end at least a few days earlier and I gave up a piece of my own thumb as an offer to “the almighty thesis”, I am very satisfied by the result of which I hope readers can enjoy as well.

Paulien Baeten

OUTLINE

LIST OF ABBREVIATIONS

ABCA1: ATP-binding cassette transporter 1
Arg1: arginase 1
AU: arbitrary unit
BMDMs: bone marrow-derived macrophages
BMS: Basso Mouse Scale
CD: cluster of differentiation
CNS: central nervous system
DMSO: dimethyl sulfoxide
dpi: days post injury
FIZZ: found in inflammatory zone
FPR2: formyl peptide receptor 2
GFAP: glial fibrillary acidic protein
GPR18: G-protein coupled receptor 18
HATs: histone acetyltransferases
HDACs: histone deacetylases
HMBS: hydroxymethylbilane synthase
Iba1: ionized calcium binding adaptor molecule 1
IFNγ: interferon γ
IgG: immunoglobulin G
IHC: immunohistochemistry
IL: interleukin
iNOS: inducible nitric oxide synthase
LPS: lipopolysaccharide
LXR: liver X receptor
MBP: myelin basic protein
MHC-II: major histocompatibility complex class II
mRNA: messenger RNA
MS: multiple sclerosis
ORO: Oil Red O
PBMCs: peripheral blood mononuclear cells
PBS: phosphate-buffered saline
PPARγ: peroxisome proliferator-activated receptor γ
qPCR: quantitative polymerase chain reaction
RNS: reactive nitrogen species
ROS: reactive oxygen species
SC debris: spinal cord debris
SCI: spinal cord injury
SDS: sodium dodecyl sulphate
SEM: standard error of mean
TBS-T: Tris-buffered saline with Tween 20
TGFβ: tumor growth factor β
TMEM119: transmembrane protein 119
TNFα: tumor necrosis factor α
w/v: percentage weight per volume
wpi: week post injury
YWHAZ: tyrosine 3-monooxygenase/tryptophan 5-monooxygenase activation protein zeta

ABSTRACT

Introduction: Spinal cord injury (SCI) is a complex disorder with high impact on the daily life of the patient. However, no effective treatment currently exists. Axonal regeneration mainly fails because of glial scar formation and excessive neuroinflammation. Infiltrating macrophages are key players in the complicated pathophysiology of SCI because of their persistence in high numbers in the lesion. Typically, macrophages are divided into two phenotypes: 1) the inflammatory M1 phenotype which is predominant during SCI and correlates with axonal dieback and 2) the transient anti-inflammatory M2 phenotype associated with axonal regeneration and neuroprotection. A lot of lipids from cellular and myelin debris are present in the lesion during SCI. They are phagocytosed by M2 macrophages in particular. When there is an overload of phagocytosed lipids, the macrophages become foamy which is phenotypically associated with the M1 phenotype. The balance of the macrophage polarization has been found to be influenced by histone deacetylase 3 (HDAC3); targeting HDAC3 can shift the polarization towards the M2 phenotype. Therefore, this study hypothesizes that inhibition of HDAC3, as a central regulator of macrophage polarization, will improve functional recovery in a mouse model of SCI.

Material & Methods: First, the phenotype of LPS- and IL-4-primed macrophages after stimulation with HDAC3 specific inhibitor RGFP966 was determined *in vitro*. Expression levels and functionality of known M1 and M2 markers and phagocytic capacity were analyzed. Next, the effect of systemic administration of RGFP966 in mice with a T-cut spinal cord hemisection injury was evaluated. The functional recovery was followed using the Basso Mouse Scale and immunohistological tissue analysis of the spinal cords was performed.

Results: *In vitro* analysis of several M1 and M2 markers reveals that RGFP966 enhances the expression and activity of M2 marker Arg1 by IL-4-primed macrophages. On the contrary, RGFP966 has no effect on the gene expression of LPS-induced M1 markers. These data indicate that RGFP966 boosts the IL-4-induced M2 phenotype of macrophages. *In vitro*, LPS- and IL-4-primed macrophages phagocytose spinal cord debris and become foamy as a result. Administration of RGFP966 reduces the formation of foamy macrophages *in vitro* regardless of their state of activation. It is not clear whether RGFP966 enables these macrophages to maintain their lipid homeostasis or whether it reduces their phagocytic ability. RGFP966 does not improve functional recovery in the mouse model of SCI nor does it modulate the macrophage polarization on acute or chronic term *in vivo*.

Conclusion: HDAC3 specific inhibitor RGFP966 has promising effects *in vitro* because it boosts the Arg1-correlated M2 phenotype of macrophages. These results strengthen our hypothesis. However, the inhibitor does not affect the functional recovery or the macrophage polarization *in vivo*. It is possible that the complex pathophysiology might overcome the potential effect of RGFP966.

Key words: spinal cord injury, neuroinflammation, macrophage polarization, HDAC3 inhibition, functional recovery

SAMENVATTING

Introductie: Dwarslaesie is een complexe aandoening met een hoge impact op het dagelijkse leven van de patiënt. Voorlopig bestaat er nog geen effectieve behandeling. Axon regeneratie faalt onder andere door vorming van het gliale litteken en neuro-inflammatie. Infiltrerende macrofagen spelen een belangrijke rol in de pathofysiologie omdat ze voor lange tijd in hoge aantallen voorkomen in het letsel. Macrofagen worden meestal ingedeeld in twee fenotypes: 1) het inflammatoire M1 fenotype dat dominant is na een dwarslaesie en correleert met het terugtrekken van de axonen en 2) het kortstondige anti-inflammatoire M2 fenotype geassocieerd met axon regeneratie. Daarnaast zijn er veel lipide resten van cellen en myeline aanwezig in het letsel die vooral gefagocyteerd worden door M2 macrofagen. Als er teveel intracellulaire lipiden zijn, kunnen de macrofagen "foamy" worden. Deze macrofagen hebben een M1-achtig fenotype. Histon deacetylase 3 (HDAC3) zou de macrofaag polarisatie kunnen beïnvloeden; inhibitie van HDAC3 kan de polarisatie naar het M2 fenotype verschuiven. Daarom is de hypothese van deze studie dat inhibitie van HDAC3, met diens controle over de macrofaag polarisatie, het functioneel herstel zal verbeteren in een muismodel van dwarslaesie.

Materiaal & Methoden: Ten eerste werd het fenotype van LPS- en IL-4-gestimuleerde macrofagen in de aanwezigheid van de HDAC3-specifieke inhibitor RGFP966 *in vitro* geïdentificeerd. Expressie en functionaliteit van gekende M1 en M2 markers en capaciteit van fagocytose werden geanalyseerd. Daarnaast werd het effect van systemische administratie van RGFP966 bekeken in muizen met een T-vormige hemisectie van het ruggenmerg. Hiervoor werd het functioneel herstel opgevolgd met behulp van de Basso Muis Schaal en werd het ruggenmerg immunohistologisch geanalyseerd.

Resultaten: *In vitro* analyse van verschillende M1 en M2 markers onthult dat RGFP966 de expressie en de activiteit van M2 marker Arg1 door IL-4-gestimuleerde macrofagen opdrijft. RGFP966 heeft integendeel geen effect op de gen expressie van LPS-geïnduceerde M1 markers. Deze resultaten impliceren dat RGFP966 het IL-4-geïnduceerde M2 fenotype boost. *In vitro* fagocytoseren LPS- en IL-4-gestimuleerde macrofagen het lipide afval van het ruggenmerg en worden hierdoor "foamy". RGFP966 vermindert het vormen van deze "foamy" macrofagen *in vitro* onafhankelijk van hun activatie status. Het is niet duidelijk of RGFP966 de macrofagen in staat stelt hun lipide homeostase te behouden of dat de inhibitor de fagocyterende capaciteit van deze macrofagen vermindert. Na behandeling met RGFP966 is er echter geen verbetering van het functioneel herstel in het muismodel van dwarslaesie en ook het macrofaag fenotype blijft onveranderd op zowel acute als chronische termijn.

Conclusie: De HDAC3-specifieke inhibitor RGFP966 heeft *in vitro* beloftevolle effecten: het boost het Arg1-gecorreleerde M2 macrofaag fenotype. Deze resultaten versterken onze hypothese. Maar de inhibitor heeft geen effect op het functioneel herstel of op de macrofaag polarisatie *in vivo*. Dit is zou het gevolg kunnen zijn van de complexe pathofysiologie waardoor het potentiële effect van RGFP966 verloren raakt.

Sleutelwoorden: dwarslaesie, neuro-inflammatie, macrofaag polarisatie, HDAC3 inhibitie, functioneel herstel

1. INTRODUCTION

1.1. Pathophysiology of spinal cord injury

Spinal cord injury (SCI) is a severe condition of the central nervous system (CNS) which can lead to permanent disability (1). Young, otherwise healthy adult men predominantly suffer from SCI (2). Causes are motor vehicle accidents, falls, violent crime, sport-related injuries or diseases (2). It results into loss of sensation and failure of motor and autonomic function at and below the level of injury (3). In addition, SCI is associated with psychological and socioeconomic impairments and long-term complications such as respiratory, cardiovascular, urinary, bowel and sexual dysfunction, spasticity and neuropathic pain (3). These complications increase the morbidity and mortality of these patients while the quality of life decreases (3). Injuries to the spine are very heterogeneous and complex, explaining the current lack of an effective treatment (1, 2). At present, the treatment of SCI consists of minimizing secondary injury by anti-inflammatory, pharmacological and surgical intervention, managing complications and improving quality of life by rehabilitation and adaptation of lifestyle (2-4).

At the onset, mechanical forces lead to primary loss of neurons, oligodendrocytes and other glial cells and disruption of blood vessels, axons and myelin sheaths (1, 2, 5, 6). These events cause early intrinsic axonal dieback (7). Immediately after the injury, the distal and proximal part of the interrupted axons separate (8). The distal part undergoes Wallerian degeneration (9). The proximal part undergoes acute axonal degeneration during which the microtubules and neurofilaments disassemble causing the axon to break up into fragments which are phagocytosed (1, 8-10). Next, the membrane seals at the cut end and forms endbulb structures (1, 8). As a result, function at and below the level of injury is immediately lost (2). The axonal interruption is the largest obstacle that has to be overcome in order to treat SCI. Following the primary injury, multicellular, cytotoxic processes are triggered (2, 4, 11). These processes, such as neuroinflammation and associated oxidative stress, ischemia, edema and glutamate excitotoxicity, result in secondary injury to tissue that initially survived (2, 4, 11). During secondary injury, cells continue to die and more axons become damaged and will retract (2, 9). Lastly, a fluid-filled cyst surrounded by a glial scar is formed (1, 2). Astrocytes are triggered to undergo reactive gliosis during which they proliferate, become hypertrophic and accumulate with meningeal cells, macrophages and microglia to create the glial scar (1, 5, 12, 13). This scar is initially beneficial by suppressing inflammation and preserving the tissue, but can eventually block axonal regeneration chemically and physically (2, 12-17). The pathophysiological process is represented in Figure 1.

Eventually, the lesion stabilizes and axonal regeneration occurs, however, without success (2). The regeneration of axons is a complex process influenced by many intrinsic factors (1, 9). First, the membrane must completely reseal. Next, the growth cone is formed by rearranging cytoskeletal proteins. Then, the

membrane is elongated by fusion of vesicles. The axon elongates in response to environmental cues and eventually forms synapses (9). If any step fails, an endbulb is formed. Organelles and fragments of the membrane accumulate in the bulb and the axon is unable to grow (9). Compared to the peripheral nervous system, the intrinsic regenerative capacity of the CNS is poor (1, 5). In addition, myelination of newly formed and spared axons is scarce since oligodendrocyte progenitor cells differentiate into astrocytes at the expense of mature oligodendrocytes to form the glial scar (5). Both remyelination and regeneration decline with age (1, 5).

Besides the intrinsic factors, axonal regeneration is influenced by extrinsic factors present in the local lesion environment during SCI as well (1). Myelin debris and the glial scar hinder axonal growth, while other chemical components of the glial scar and neurotrophic factors can stimulate repair (1, 5, 12, 15-18). Neuroinflammation has both supportive and detrimental effects on the axonal regeneration which will be discussed in the next chapter (5, 7, 11, 19-22).

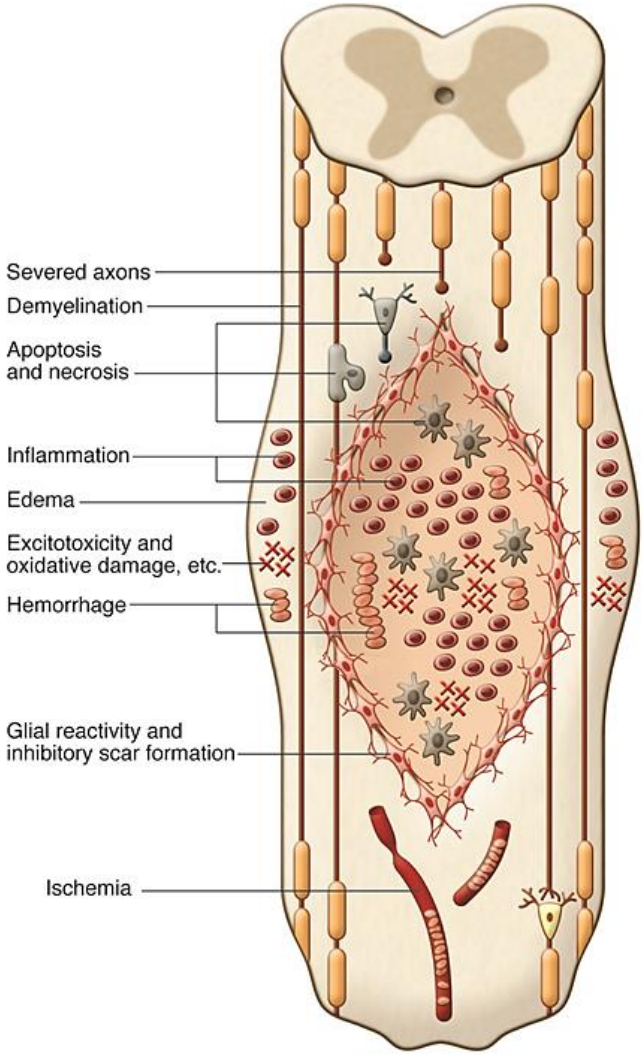

Figure 1: The pathophysiology of spinal cord injury. At the onset, the primary mechanical forces lead to apoptosis and necrosis of neurons and glial cells, severing and demyelination of axons and disruption of blood vessels causing hemorrhages. This primary injury triggers cytotoxic processes such as inflammation and associated oxidative stress, ischemia, edema and glutamate excitotoxicity. Lastly, a glial scar is formed. (Modified from (23))

1.2. Neuroinflammation

Neuroinflammation can reestablish tissue homeostasis, however, it can cause secondary injury as well (5, 11, 14, 19, 21, 22). Apoptotic and necrotic cells activate resident microglia, the first to respond to the injury (Figure 2), leading to production of chemokines, cytokines and free radicals (20, 24, 25). Permeability of blood vessels is increased because of the primary disruption and oxidative damage of the endothelial cells while the expression of cell adhesion molecules is stimulated (2, 11, 24). Altogether, this causes the recruitment of peripheral leukocytes to the injured spinal cord (11, 25-27). They produce cytokines and chemokines themselves and a self-sustainable cycle is created (26, 27). Neutrophils infiltrate the lesion site first, followed by the monocyte-derived macrophages and lymphocytes (Figure 2) (20, 28). Together, macrophages and neutrophils have a non-specific activity by which they clear cellular and tissue debris which is beneficial since it creates a suitable environment for regeneration (1, 11, 19, 28-30). In addition, neutrophils release angiogenic factors (30). But when left uncontrolled, the neutrophils and macrophages can damage the tissue (1, 11, 19, 28-30). During SCI, the attracted macrophages persist in large numbers in the lesion core, making them one of the most important cell types involved in the pathological process (11, 31, 32). Resident microglia on the contrary, reside on the edges of the lesion and in the uninjured areas where they seal the lesion and prevent spreading of damage (32, 33).

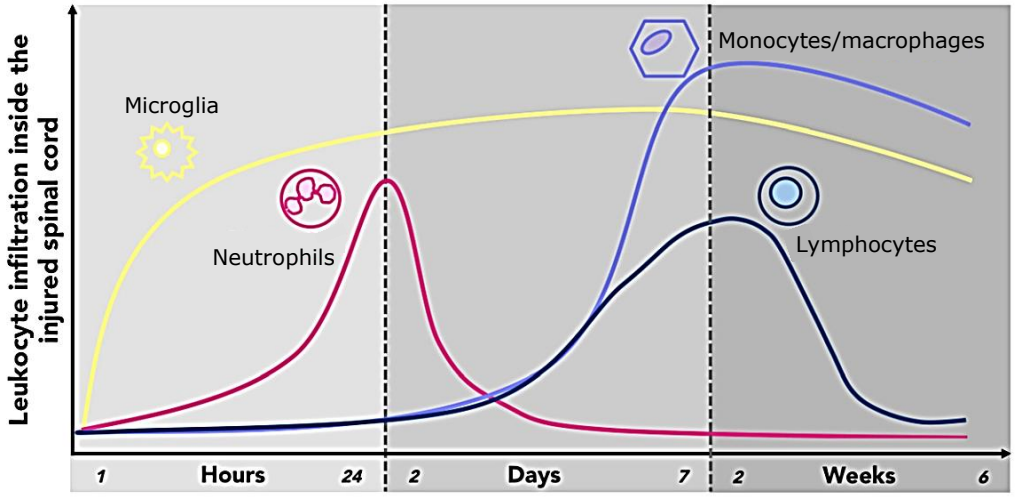

Figure 2: The timing of immune cell infiltration into the injured spinal cord. Resident microglia first respond to the injury and remain activated. Next, neutrophils infiltrate transiently followed by lymphocytes and high numbers of persistent monocyte-derived macrophages. (Modified from (20))

Depending on the microenvironment, consistent of cytokines and lesion-related factors, the macrophages differentiate towards the classically activated, pro-inflammatory M1 phenotype or the alternatively activated, anti-inflammatory M2 phenotype (19). The M1 macrophages, induced by interferon γ (IFNγ), tumor necrosis factor α (TNFα) or activation of toll-like receptors, mediate a pro-inflammatory response which is involved in host defense and tumor cell killing but collateral damage to healthy tissue is possible (19, 34). During SCI, M1 macrophages cause a chronic inflammatory response and act neurotoxic since they produce cytokines, reactive

oxygen and nitrogen species (ROS and RNS) and proteolytic enzymes (19, 21, 35). Experimental models of SCI show that the timing of macrophage infiltration correlates with axonal dieback which is independent of the intrinsic axonal retraction (7, 8). This secondary phase in axonal retraction is caused by cell-cell interactions between dystrophic axons and M1 macrophages (6, 7, 36). Macrophages secrete proteases which cause the axons to lose adhesion with the substrate resulting in dieback (7).

On the contrary, the M2 macrophages are induced by interleukin-4 (IL-4), IL-13, IL-10 or tumor growth factor β (TGFβ) and promote wound healing and angiogenesis while suppressing the immune system (19, 34, 37, 38). During SCI, the M2 macrophages create a supportive environment for axonal regeneration by phagocytosing cellular and myelin debris (19, 39). The phagocytosed lipids activate nuclear receptors liver X receptor (LXR) and peroxisome proliferator-activated receptor γ (PPARγ) to further trigger the M2 phenotype and promote the lipid metabolism (40, 41). In co-culture with neurons, the M2 macrophages stimulate unipolar or bipolar neurite outgrowth even in an inhibitory environment (19). In addition, these macrophages are neuroprotective and release neurotrophic factors (19, 20, 35, 37, 42). In experimental models of neuroinflammation, M2 macrophages are shown to enhance oligodendrocyte differentiation and preservation and thereby promote remyelination (39, 43). In general, the M2 macrophages are associated with functional recovery.

These described phenotypes are opposite extremes, however, cells can have mixed phenotypes *in vivo* and are able to adapt their phenotype and function in response to the environment (19, 34, 44). At the onset, both M1 and M2 macrophages are present in the lesion during SCI, but the anti-inflammatory M2 macrophages disappear quickly, while the pro-inflammatory M1 macrophages persist for at least one month (5, 19, 32, 45). This is due to cues in the lesion environment which favor the differentiation of infiltrated and newly infiltrating macrophages towards the M1 phenotype and suppress differentiation towards the M2 phenotype (19, 45). In the injured spinal cord, levels of M1 phenotype-promoting factors IFNγ and TNFα are high while levels of M2 phenotype-promoting factors IL-4, IL-13, IL-10 are very low (19, 46). In addition, the presence of foamy, lipid-laden macrophages correlates with the disappearance of the M2 macrophages (32, 47). M2 macrophages phagocytose the tissue debris and degrade it into neutral lipids (32). But when there is an overload of debris, it persists in the lesion site during SCI for a long time, foamy macrophages with a M1-like phenotype and decreased phagocytic ability are formed (32, 47). The expression of ATP-binding cassette transport A1 (ABCA1) is decreased in these cells leading to a failure of the lipid homeostasis (32). The lipids are no longer transported out of the cells and this causes the lipid accumulation (32).

Because of the predominant presence of M1 macrophages, global depletion or functional inhibition of macrophages has been found to be neuroprotective and to promote functional recovery in different experimental models of SCI (19, 21, 22, 48). However, the supportive M2 macrophages are also lost. Indeed, this happens during the anti-inflammatory treatment standardly used after SCI as well (11, 48). Therefore, a way must be found to decrease detrimental inflammation caused by M1 macrophages while the M2 macrophage response is enhanced regardless of the lesion environment during SCI. Macrophages can switch

between phenotypes and this ability can be used as a therapeutic target (49). Preliminary data from our research group and previous research have shown that administration of M2-inducing cytokines IL-4, IL-10 and IL-13 to macrophages in co-culture with neurons, improves neuronal survival and neurite growth (19). Moreover, these cytokines improve functional recovery in animal models of SCI as demonstrated by our research group; administration of IL-13-producing mesenchymal stem cells to mice with a T-cut spinal cord hemisection injury increases the presence of M2 macrophages *in vivo* and improves the functional recovery (50). These results suggest that the M2 macrophages indeed stimulate axonal regeneration and thereby improve functional recovery; however, these cytokines have broad-acting and transient effects.

1.3. Histone deacetylase inhibitors

Another way to induce the M2 phenotype is to make use of epigenetic modulation since the transcriptional program differs between M1 and M2 macrophages. During this epigenetic modulation, enzymes work together to change the chromatin in order to control the gene expression for each cell type specifically without changing the DNA sequences themselves (5, 51). For instance, these enzymes can create histone methylation or acetylation (51). Histone acetyltransferases (HATs) acetylate lysine residues of N-terminal tails of histones to induce gene expression (Figure 3A) (5, 51). Histone deacetylases (HDACs) remove the acetyl group; the chromatin becomes more compact and the gene expression is suppressed (Figure 3A) (5, 51).

HATs and HDACs play an important role during SCI since a global, significant reduction in acetylation levels in animal models has been observed (5, 52, 53). This could be the result of an increased activity of HDACs and therefore, inhibition of HDACs could restore this imbalance (Figure 3B). Therefore, many HDAC inhibitors have already been used in research on neuroinflammation, next to their clinical use in epilepsy, bipolar disorder and cancer treatment (54, 55). A non-specific HDAC inhibitor, valproic acid, improves functional recovery after SCI in many experimental models (52, 53, 56). It is found to be neuroprotective by reducing apoptotic cell death, inflammation and secondary damage (52, 56). However, it is not yet known which HDAC isoform is responsible for the effect since there exist four classes in the HDAC family (51). In humans, the gene and protein expression of HDAC3 of peripheral blood mononuclear cells (PBMCs) is increased in patients with SCI (57). Research has found that HDAC3 plays in important role in inflammation during SCI (5, 58, 59). It has been identified as an epigenomic brake in alternative activation of macrophages *in vitro* and *in vivo* (59). Deletion of HDAC3 impairs lipopolysaccharide (LPS)-stimulated gene expression of inflammatory genes by M1 macrophages and shifts gene expression towards that seen in alternative activation (58, 59). In addition, responsivity of HDAC3-deficient macrophages to IL-4 stimulation is increased (58). Scriptaid, an HDAC1, HDAC3 and HDAC8 inhibitor, has already been used in experimental traumatic brain injury, which is characterized by excessive neuroinflammation like SCI (39). *In vivo*, Scriptaid shifts the microglial and macrophage polarization towards the M2 phenotype (39). As a result, inflammation is suppressed and oligodendrocytes are spared which

ultimately leads to preservation of white matter and nerve conduction (39). A mouse model with myeloid cell-specific knockout of HDAC3 (HDAC3$^{flox/flox}$;LysMCre) has already been used to study the effect on atherosclerosis (60). The HDAC3-deficient macrophages are mainly differentiated towards the M2 phenotype and thereby the outcome is improved *in vivo* (60). However, specific targeting of HDAC3 in the macrophages has never been previously studied in any experimental model of SCI.

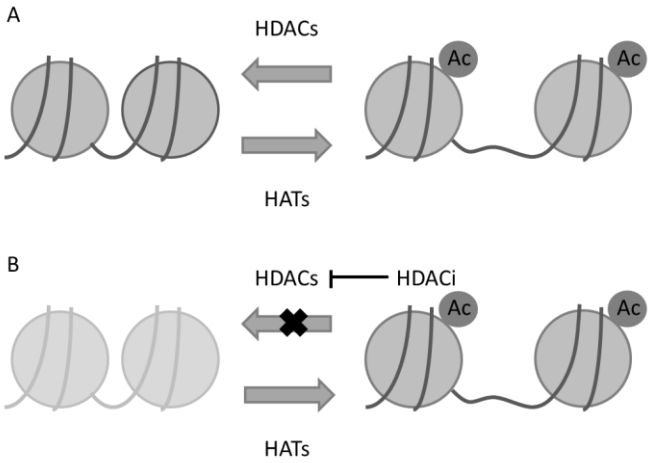

Figure 3: Acetylation and deacetylation of histones by HATs and HDACs and the effect of an HDAC inhibitor. (A) Under normal circumstances, histone acetyltransferases (HATs) acetylate histones, making the chromatin more relaxed (right). Histone deacetylases (HDACs) remove acetyl groups from histones, making the chromatin more compact (left). (B) Using an HDAC inhibitor (HDACi), deacetylation of histones is prevented and acetylation levels increase. Thereby, gene expression is stimulated (right).

1.4. Research aims

Literature shows that inhibition of HDAC3 drives macrophage polarization away from the inflammatory M1 phenotype and towards the anti-inflammatory M2 phenotype. In addition, the M2 phenotype is associated with axonal regeneration after SCI. Therefore, it is hypothesized that inhibition of HDAC3, as a central regulator of macrophage polarization, will improve functional recovery in a mouse model of SCI.

To evaluate the effect of HDAC3 specific inhibitor RGFP966 on the macrophages, the phenotype of LPS- and IL-4-primed macrophages after stimulation with RGFP966 was identified *in vitro*. Results show that RGFP966 enhances IL-4-induced Arg1 expression and functionality. No effect of RGFP966 is observed on the gene expression of LPS-induced factors. In addition, RGFP966 reduces the formation of foamy macrophages regardless of their state of activation. To validate the effect on the functional recovery, mice with a T-cut spinal cord hemisection injury were treated with RGFP966. The functional recovery *in vivo* was followed using Basso Mouse Scale and spinal cords were histologically analyzed at different time points. Results show that RGFP966 does not improve functional recovery in the experimental model of SCI. The macrophage polarization *in vivo* is not changed on acute nor on chronic term. It is likely that the potential effect of RGFP966 gets lost in the complex pathophysiology of SCI.

2. MATERIALS AND METHODS

2.1. *In vitro* experiments

2.1.1. Isolation and differentiation of bone marrow-derived macrophages

Bone marrow was isolated from femurs and tibias from female Balb/c mice (Envigo, Cambridgeshire, U.K.) as previously described (7). The isolated monocytes were differentiated towards primary macrophages using RPMI (Lonza, Bazel, Switzerland) supplemented with 15% L929-conditioned medium, 10% fetal calf serum (Gibco (Thermo Fisher Scientific), Waltham, U.S.A.) and 1% penicillin/streptomycin (Sigma-Aldrich, Saint Louis, U.S.A.) for ten days. One day before stimulation, the bone marrow-derived macrophages (BMDMs) were plated.

2.1.2. Treatment of bone marrow-derived macrophages

The BMDMs were activated with IL-4 (30 ng/ml, Peprotech, Rocky Hill, U.S.A.) to represent M2 macrophages or LPS (200 ng/ml, EMD Millipore, Billerica, U.S.A.) to represent M1 macrophages. One hour later, BMDMs were stimulated with only dimethylsulfoxide (DMSO) (Sigma-Aldrich) as a control or HDAC3 specific inhibitor RGFP966 (5 μM or 10 μM in DMSO, Cayman Chemicals, Ann Arbor, U.S.A) for 24 hours. The macrophages were handled differently in the following steps.

The BMDMs were directly lysed using β-mercaptoethanol in RLT-buffer (1:100, RNeasy Mini Kit, Qiagen, Hilden, Germany) or sodium dodecyl sulphate (SDS) lysis buffer (2% (w/v) in 125 mM Tris) to isolate messenger RNA (mRNA) or proteins respectively. Cell pellets for the arginase activity assay were obtained using centrifugation (10 minutes at 1000 g). The timeline is represented in Figure 4.

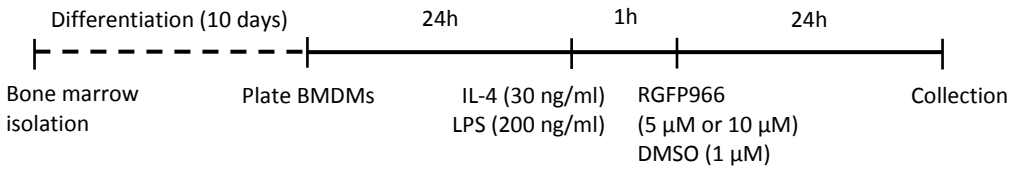

Figure 4: Timeline of the *in vitro* experiments. Bone marrow was isolated from female Balb/c mice and differentiated into bone marrow-derived macrophages (BMDMs) for ten days. BMDMs were plated 24 hours before stimulation with IL-4 or LPS. One hour later, the cells were stimulated with only DMSO as a control or RGFP966 in two concentrations. After 24 hours, the cells were processed according to the required experiments. Proteins or mRNA were isolated from these cells or cell pellets were collected. IL-4: interleukin-4; LPS: lipopolysaccharide; DMSO: dimethylsulfoxide

Alternatively, spinal cord debris (50 µg) was added to the stimulated cells two times separated by 24 hours. Spinal cords were isolated from female Balb/c mice (Envigo) and snap-frozen in liquid nitrogen. Tissue was grinded using a TissueRuptor (Qiagen) and a 70 µm strainer. Debris was resolved in phosphate-buffered saline (PBS, 1X). Conditions without spinal cord debris were used as controls. The stimulated cells were fixated using 4% paraformaldehyde. To identify foamy macrophages, an Oil Red O staining was performed. The timeline of this experiment is illustrated in Figure 5.

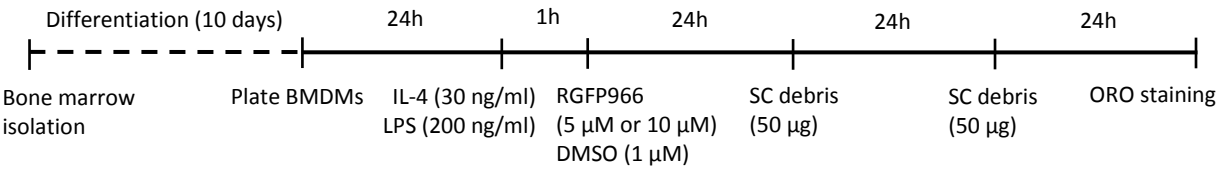

Figure 5: Timeline of the *in vitro* experiments. Bone marrow was isolated from female Balb/c mice and differentiated into bone marrow-derived macrophages (BMDMs) for ten days. BMDMs were plated 24 hours before stimulation with IL-4 or LPS. One hour later, the cells were stimulated with HDAC3 inhibitor RGFP966 or only DMSO as a control. Next, spinal cord debris (SC debris) was added to the cells two times separated by 24 hours. Lastly, the cells were used for an Oil Red O (ORO) staining. IL-4: interleukin-4; LPS: lipopolysaccharide; DMSO: dimethylsulfoxide

2.1.3. Quantitative polymerase chain reaction

To measure the gene expression, quantitative polymerase chain reaction (qPCR) was used. Cell lysis was performed with β-mercaptoethanol in RLT-buffer (1:100, RNeasy Mini Kit, Qiagen) on stimulated cells. mRNA was isolated using RNeasy Mini Kit (Qiagen) following manufacturer's instructions and the mRNA concentration was measured with Nanodrop (Thermo Fisher Scientific). cDNA was created with qScript cDNA Supermix according to manufacturer's instructions (Quanta Biosciences, Gaithersburg, U.S.A.). Fast SYBR Green Master Mix (1X, Life Technologies, Carlsbad, U.S.A.) was used in combination with sample cDNA (12,5 ng), forward and reverse primers (0,3 µM each, Supplementary Table 1) and RNase free water to make a total reaction volume of 10 µl on which a quantitative measurement of gene expression with StepOne Software (Thermo Fisher Scientific) was performed (1 cycle of 20 seconds at 95°, 40 cycles of 3 seconds at 95°C and 30 seconds at 60°C, 1 cycle of 15 seconds at 95°C, 60 seconds at 60°C and 15 seconds at 95°C). Relative quantification of gene expression was accomplished by using the comparative Ct method. Data were normalized to the most stable reference genes using geNorm.

2.1.4. Western blot

Stimulated BMDMs were lysed in SDS lysis buffer (2% (w/v) in 125 mM Tris) to isolate proteins. Using Pierce BCA protein assay (Thermo Fisher Scientific) according to manufacturer's instructions and iMARK Microplate Reader (Bio-Rad Laboratories, Hercules, U.S.A.), protein concentrations were measured. Samples (10 µg) were

separated on 12% SDS gels at 200V in running buffer (25 mM Tris, 192 mM glycine, 0,1% SDS, pH 8,3). Proteins were transferred by wet transfer to a PVDF membrane (Merck Millipore, Amsterdam, The Netherlands) for 90 minutes at 350mA in transfer buffer (26,4 mM Tris, 197 mM glycine, 10% methanol). Non-specific binding was blocked using 5% (w/v) milk powder in Tris-buffered saline with Tween 20 (TBS-T) (20 mM Tris, 137 mM NaCl, 0,1% Tween 20, pH 7,6) for one hour and the membrane was incubated with primary antibodies targeting mouse Arg1 (1/1000, Santa Cruz Technologies, Dallas, U.S.A.) at 4°C overnight or mouse β-actin (1/2000, Santa Cruz Technologies) at room temperature for one hour. Next, the membranes were incubated with corresponding secondary antibodies labeled with horseradish peroxidase (1/2000, Dako, Santa Clara, U.S.A.) for one hour at room temperature. Pierce ECL Western Blotting Substrate (Thermo Fisher Scientific) was used following manufacturer's instructions to develop an image using Image Quant LAS 4000 mini (GE Healthcare Life Sciences, Little Chalfont, U.K.). The measured values of Arg1 were normalized to the level of β-actin.

2.1.5. Arginase activity assay

Cell pellets were created by centrifugation for 10 minutes at 1000 g and used to measure arginase activity with the arginase activity assay kit (Sigma-Aldrich) according to manufacturer's instructions. This assay colorizes urea produced by arginase which converses L-arginine into urea and L-ornithine and represents the enzymatic activity of arginase.

2.1.6. Oil Red O staining

Stimulated cells were fixated using 4% paraformaldehyde. Before and after staining with Oil Red O working solution (0,30% (w/v) Oil Red O in 60% isopropanol), cells were incubated with 60% isopropanol. The staining was extracted using 100% isopropanol and measured at 490 nm using iMARK Microplate Reader (Bio-Rad Laboratories). The staining intensity was normalized to the number of cells present per well.

2.2. Animal experiments

2.2.1. Animals

Experiments were performed using 10-week old female Balb/c mice (Envigo). The animals were housed in groups under regular conditions (temperature- and humidity-controlled, 12-hour light/dark cycle and food and water *ad libitum*) in a conventional animal facility at Hasselt University. All experiments were performed according to the guidelines described in Directive 2010/63/EU and were approved by the local ethical committee of Hasselt University.

2.2.2. T-cut spinal cord hemisection injury

T-cut spinal cord hemisection injury was performed as described before (61, 62). 10-week old female mice underwent a partial laminectomy at thoracic level T8 under anesthesia. Iridectomy scissors were used to transect left and right dorsal funiculus, the dorsal horns and the ventral funiculus. This procedure results in a complete transection of the dorsomedial and ventral corticospinal tract and causes dysfunction of several other descending and ascending tracts. The muscles were sutured and the back skin was closed with wound clips. Animals received an injection of buprenorphine hydrochloride (8 ng/mouse) subcutaneously next to the lesion and glucose (20%) intraperitoneally. Enrofloxacine (2%) was added in the drinking water for the first week. Bladders were manually emptied daily until autonomic control was restored. Some animals were sacrificed three days post injury (3 dpi) to analyze the acute effects of the treatment. Other animals are followed-up using the Basso Mouse Scale for four weeks (4 wpi) to determine the chronic effects. The timeline of this experiment is illustrated in Figure 6.

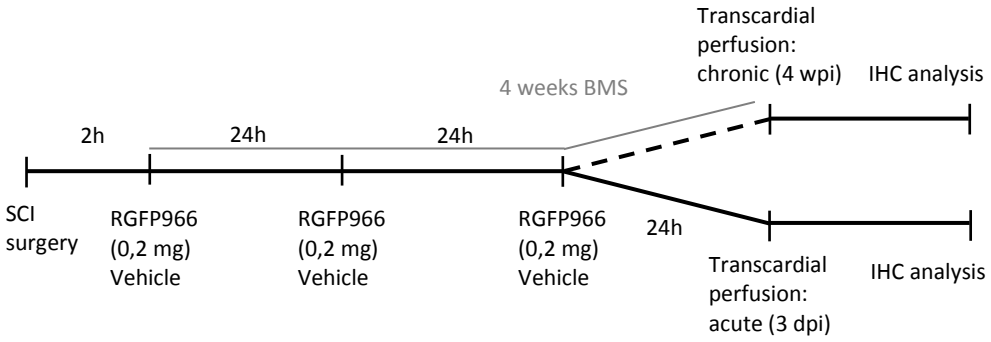

Figure 6: Time line of the *in vivo* experiments. 10-week old female Balb/c mice underwent a T-cut spinal cord hemisection injury (SCI surgery). HDAC3 inhibitor RGFP966 (0,2 mg/mouse/day) or vehicle solution (vehicle) was injected intraperitoneal on three consecutive time points after surgery. Three days after injury (3 dpi), some animals were sacrificed to analyze the effect of RGFP966 administration on the acute pathology. For four weeks, animals were scored using the Basso Mouse Scale (BMS). During the first week, animals were scored every day. During the last three weeks, the animals were scored every other day. Four weeks after injury (4 wpi), animals are sacrificed to analyze the effect of RGFP966 on chronic pathology. Longitudinal spinal cord cryosections (10 µm) were obtained from animals transcardially perfused and used for immunohistochemical (IHC) analysis.

2.2.3. Administration of HDAC3 inhibitor RGFP966

HDAC3 specific inhibitor RGFP966 (Cayman Chemical) was dissolved in DMSO (Sigma-Aldrich) and 10% diluted in 30% (w/v) hydroxypropyl-beta-cyclodextrin (SanBio, Uden, The Netherlands) in sodium acetate (100mM, pH 8) by adding it dropwise while vortexing. Animals received an intraperitoneal injection of RGFP966 (0,2 mg/mouse/day) on three consecutive time points starting two hours after surgery (Figure 6). Control animals were only treated with vehicle solution.

2.2.4. Locomotion test

Functional recovery of mice with SCI was evaluated using to the Basso Mouse Scale starting one day after injury for four weeks (Figure 6) (63). In the first week, mice were scored daily and in the last three weeks every other day. The Basso Mouse Scale is a 10-point scale (0: complete hind limb paralysis; 9: normal locomotion) of the locomotion of the hind limb movements. The mice were scored by two blinded investigators in an open field during a four minute interval.

2.2.5. Immunohistochemical analysis of spinal cords

Three days or four weeks after injury, animals were anesthetized by intraperitoneal injection of pentobarbitone sodium (8 mg/animal) followed by transcardial perfusion with ringer-heparin and 4% paraformaldehyde (Figure 6). Spinal cords were dissected and stored in sucrose (5% (w/v) in 4% paraformaldehyde) overnight at 4°C followed by several days of cryoprotection at 4°C in sucrose (30% (w/v) in 1X PBS). Spinal cords were frozen in optimal cutting temperature compound on liquid nitrogen. Longitudinal spinal cord cryosections (10 µm) were obtained.

The cryosections were blocked in corresponding serum (10%) or protein block (10%, Dako). Optionally, permeabilization was performed using 0,1% Triton-X100. The cryosections were incubated overnight at 4°C with following primary antibodies: goat anti-Arg1 (1/50, Santa Cruz Technologies), rabbit anti-TMEM119 (1/100, Abcam, Cambridge, U.K.), rat anti-MHC-II (1/200, Santa Cruz Technologies), rabbit anti-Iba1 (1/350, Wako Chemicals GmbH, Neuss, Germany), goat anti-Iba1 (1/1000, Abcam), rat anti-CD4 (1/25, BD Biosciences, San Jose, U.S.A.), mouse anti-GFAP (1/500, Sigma-Aldrich) and rat anti-MBP (1/250, EMD Millipore). Next, cryosections were incubated for one hour at room temperature with the corresponding secondary antibodies: donkey anti-goat IgG Alexa Fluor 555 and 488 (1/400, Invitrogen, Carlsbad, U.S.A.), donkey anti-rabbit IgG Alexa Fluor 555, (1/400, Invitrogen), rabbit anti-rat biotin (1/400, Dako) and streptavidin 488 (1/2000, Invitrogen), goat anti-rabbit Alexa Fluor 488 (1/250, Invitrogen), goat anti-rat IgG Alexa Fluor 568 and 488 (1/250, Invitrogen) and goat anti-mouse Alexa Fluor 568 (1/250, Invitrogen). All slides were mounted with fluorescent mounting medium (Dako). Fluorescent images were taken using a Leica fluorescence microscope (Wetzlar, Germany).

2.3. Statistical analysis

Data were reported as mean ± standard error of the mean (SEM) and statistically analyzed using GraphPad Prism (GraphPad Software, La Jolla, U.S.A.). D'Agistino and Pearson omnibus normality test was used to test

normal distribution. Two-way ANOVA combined with Tukey's multiple comparison were used if data were normally distributed. Kruskal-Wallis with Dunn's multiple comparison was used if normality was not achieved. Student's t-test was used to compare two groups. Tests were two-tailed and differences were considered significant at $p < 0,05$ (*) and $p < 0,01$ (**).

3. RESULTS

In this study, it is hypothesized that inhibition of HDAC3, as a central regulator of macrophage polarization, will improve functional recovery in a mouse model of SCI.

First, the macrophage phenotype of LPS- and IL-4-primed BMDMs after stimulation with HDAC3 specific inhibitor RGFP966 was determined *in vitro*. Results show that the IL-4-induced expression and activity of Arg1 is enhanced by RGFP966. In contrast, the LPS-induced gene expression of M1 markers is not affected by RGFP966. Next, the phagocytic capacity of the macrophages after stimulation with RGFP966 was evaluated. The HDAC3 inhibitor reduces the formation of foamy macrophages in the presence of spinal cord debris regardless of their state of activation.

Lastly, the effect of systemic administration of RGFP966 in mice with a T-cut spinal cord hemisection injury was studied. The functional recovery was followed using the Basso Mouse Scale and spinal cords were immunohistologically analyzed. The functional recovery is not improved by treatment with RGFP966. The macrophage polarization *in vivo* is unchanged after treatment with RGFP966 on the acute and long term.

3.1. RGFP966 enhances Arg1 expression by IL-4-primed macrophages *in vitro*

To evaluate the effect of HDAC3 specific inhibitor RGFP966 on the macrophage phenotype in specific, *in vitro* experiments were performed. In this study, BMDMs were stimulated with either IL-4 or LPS to prime the macrophages as M2 or M1 respectively, followed by stimulation with RGFP966 (Figure 4).

Gene expression of known M1 and M2 markers by the macrophages was analyzed. The gene expression of M2 genes Arg1 and Ym1a significantly increases by IL-4-primed macrophages after stimulation with RGFP966 compared to stimulation with IL-4 alone (Figure 7A+B). M2 marker FIZZ and M1 markers CD38, iNOS, GPR18, FPR2, IL-1β and IL-6 do not show significant differences in the presence of RGFP966 (Figure 7C-I).

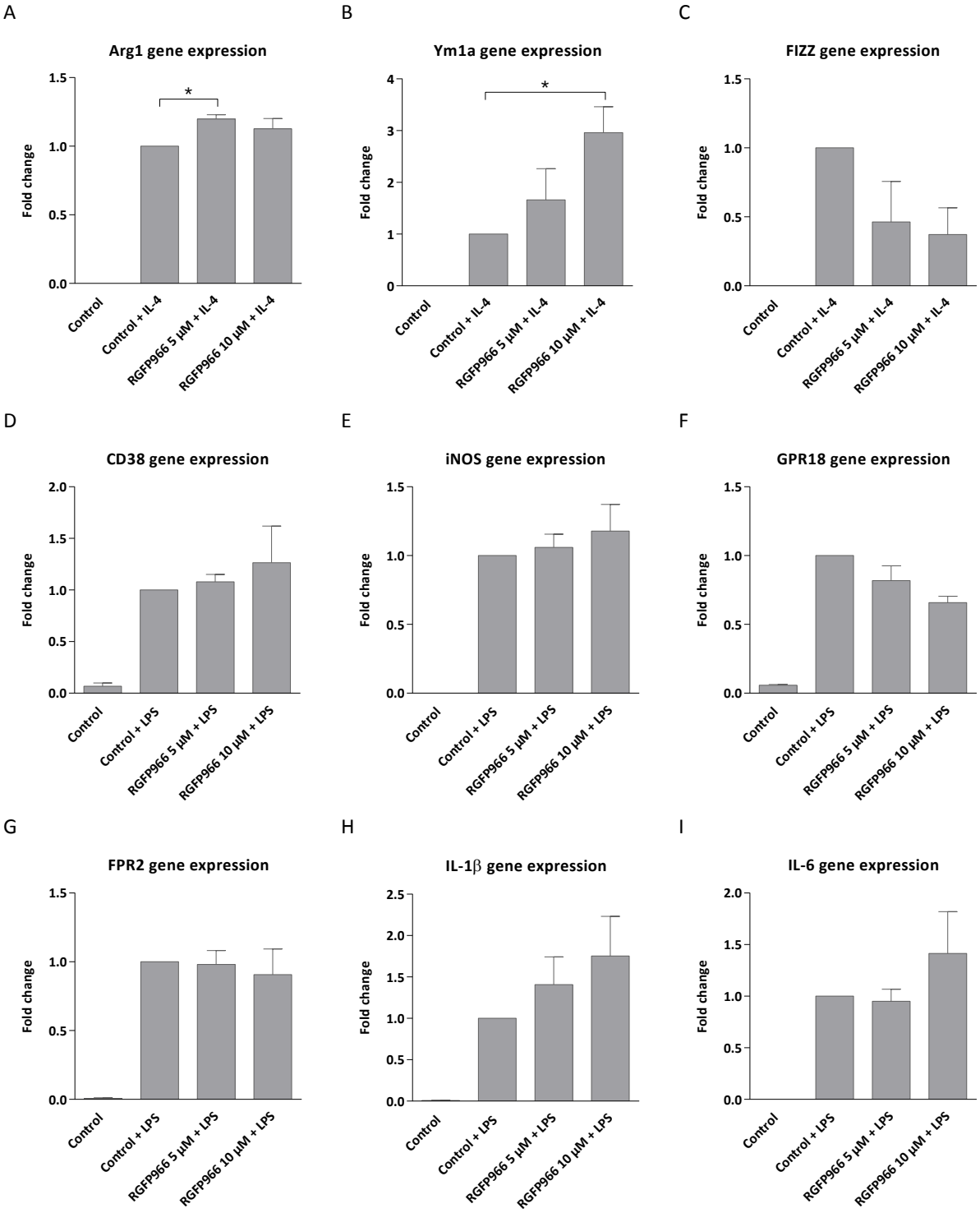

Figure 7: Stimulation of primed M1 and M2 macrophages with RGFP966 significantly increases IL-4-induced gene expression of M2 markers Arg1 and Ym1a but does not change expression of other M2 markers or LPS-induced M1 markers *in vitro*. Macrophages were primed with IL-4 or LPS before stimulation with RGFP966 and analyzed for gene expression of M2 markers Arg1 (A), Ym1a (B), FIZZ (C) and M1 markers CD38 (D), iNOS (E), GPR18 (F), FPR2 (G), IL-1β (H) and IL-6 (I). Fold change is based on only IL-4 stimulation for the M2 genes or only LPS stimulation for the M1 genes. (n=3, Kruskal-Wallis with multiple comparison, * p<0,05). IL-4: interleukin-4; LPS: lipopolysaccharide; Arg1: arginase 1; FIZZ: found in inflammatory zone; CD38: cluster of differentiation 38; iNOS: inducible nitric oxide synthase; GPR18: G-protein coupled receptor 18; FPR2: formyl peptide receptor 2; IL-1β: interleukin-1β; IL-6: interleukin-6

In addition to the gene expression of Arg1, the protein expression and functional activity of Arg1 were studied as well. RGFP966 stimulation of IL-4-primed BMDMs significantly increases protein expression of Arg1 (Figure 8A and Supplementary Figure 1). Cell pellets of IL-4-stimulated macrophages in the presence of RGFP966 were used in an arginase activity assay. RGFP966 tends to increase Arg1 activity compared to stimulation with IL-4 alone (Figure 8B). This result is preliminary and therefore, needs to be repeated to verify the result. Together, these *in vitro* results indicate that RGFP966 boosts the M2 phenotype of macrophages characterized by Arg1.

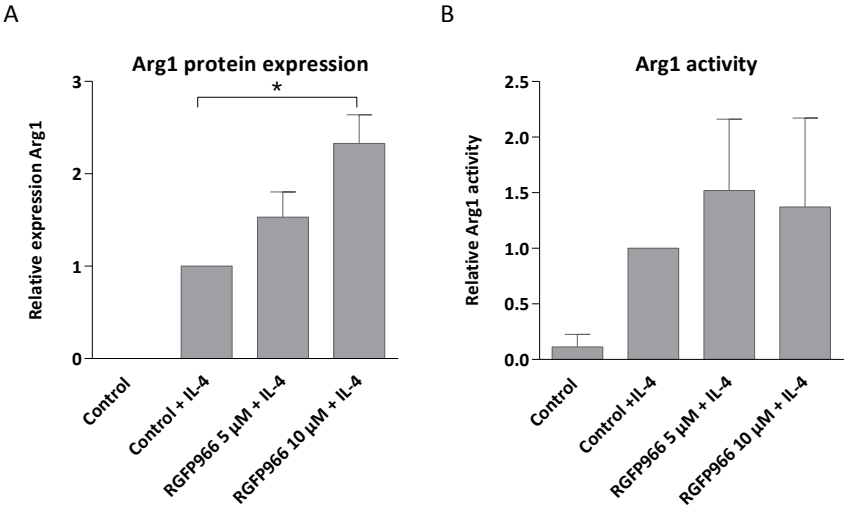

Figure 8: RGFP966 significantly increases Arg1 protein expression and tends to increase Arg1 activity of IL-4-primed macrophages *in vitro*. Macrophages were primed with IL-4 before stimulation with RGFP966. (A) The cells were analyzed for protein expression of M2 marker Arg1. Relative expression is based on only IL-4 stimulation. Expression is normalized to β-actin expression (see Supplementary Figure 1). (n=4, Kruskal-Wallis with multiple comparison, * $p<0,05$). (B) The activity of Arg1 was measured using an arginase activity assay. Relative activity is based on activity of only IL-4 stimulation. (n=2). IL-4: interleukin-4; Arg1: arginase 1

3.2. RGFP966 reduces the formation of foamy macrophages *in vitro*

To represent macrophages of the lesion environment during SCI, the BMDMs were stimulated with spinal cord debris for 48 hours next to the treatment with cytokines IL-4 and LPS and HDAC3 inhibitor RGFP966 (Figure 5).

Both M1 and M2 macrophages are turned into foamy macrophages in the presence of spinal cord debris for 48 hours (Figure 9A+B and Supplementary Figure 2A-F). Stimulation with RGFP966 at the highest concentration significantly decreases the presence of foamy macrophages of both IL-4- and LPS-primed BMDMs (Figure 9A+B and Supplementary Figure 2A-F). Spinal cord debris itself is an activator of the macrophages since naïve macrophages become foamy as well (Figure 9A-C and Supplementary Figure 2A+D+G). Therefore, macrophages were only stimulated with RGFP966 in combination with spinal cord debris for 48 hours. Again, RGFP966 significantly decreases the formation of foamy macrophages (Figure 9C and Supplementary Figure 2G-I). Consequently, RGFP966 reduces the formation of foamy macrophages independently of their activation state.

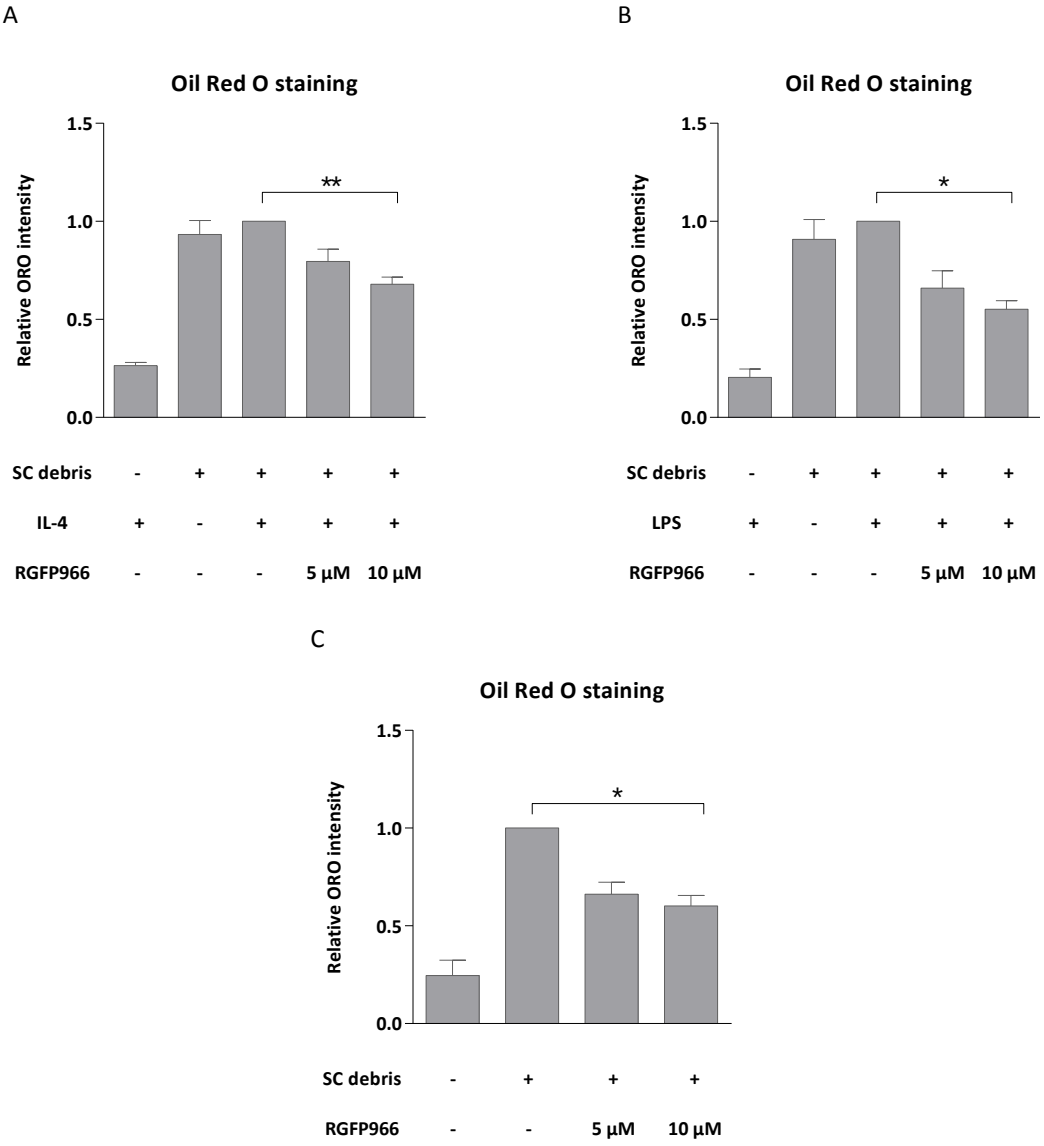

Figure 9: RGFP966 reduces the formation of naïve, LPS- and IL-4-primed macrophages into foamy macrophages in the presence of spinal cord debris for 48 hours *in vitro*. Macrophages were primed with IL-4 (A) or LPS (B) or left unstimulated (C) before stimulation with RGFP966. Next, cells were stimulated with spinal cord debris (SC debris) for two days followed by an Oil Red O (ORO) staining. Relative intensity of absorbance of the ORO staining is based on only IL-4 stimulation. Staining intensity is normalized to number of cells (represented in Supplementary Figure 2). (n=4 (IL-4), n=4 (LPS) and n=3 (unstimulated), Kruskal-Wallis with multiple comparison, * p<0,05, ** p<0,01). IL-4: interleukin-4; LPS: lipopolysaccharide

3.3. Functional recovery after spinal cord injury is not affected by treatment with RGFP966

This study investigates the effect of systemic administration of HDAC3 specific inhibitor RGFP966 on the recovery four weeks after T-cut spinal cord hemisection injury in 10-week old female Balb/c mice (Figure 6).

The functional recovery, analyzed using the Basso Mouse Scale, does not significantly increase after treatment with RGFP966 compared to the control group (Figure 10A). On histological level, the results are similar. The

lesion size, lineated by GFAP-positive perilesional astrocytes, does not significantly differ after treatment with RGFP966 (Figure 10B). The demyelinated area, a MBP-negative area, is the same in both groups (Figure 10C). Infiltration of the immune cells is represented by CD4-positive T cells and macrophages (see section 3.4). The T cell infiltration into the lesion is comparable between the groups (Figure 10D). These *in vivo* results suggest that treatment with RGFP966 is unable to improve the functional recovery of mice with SCI.

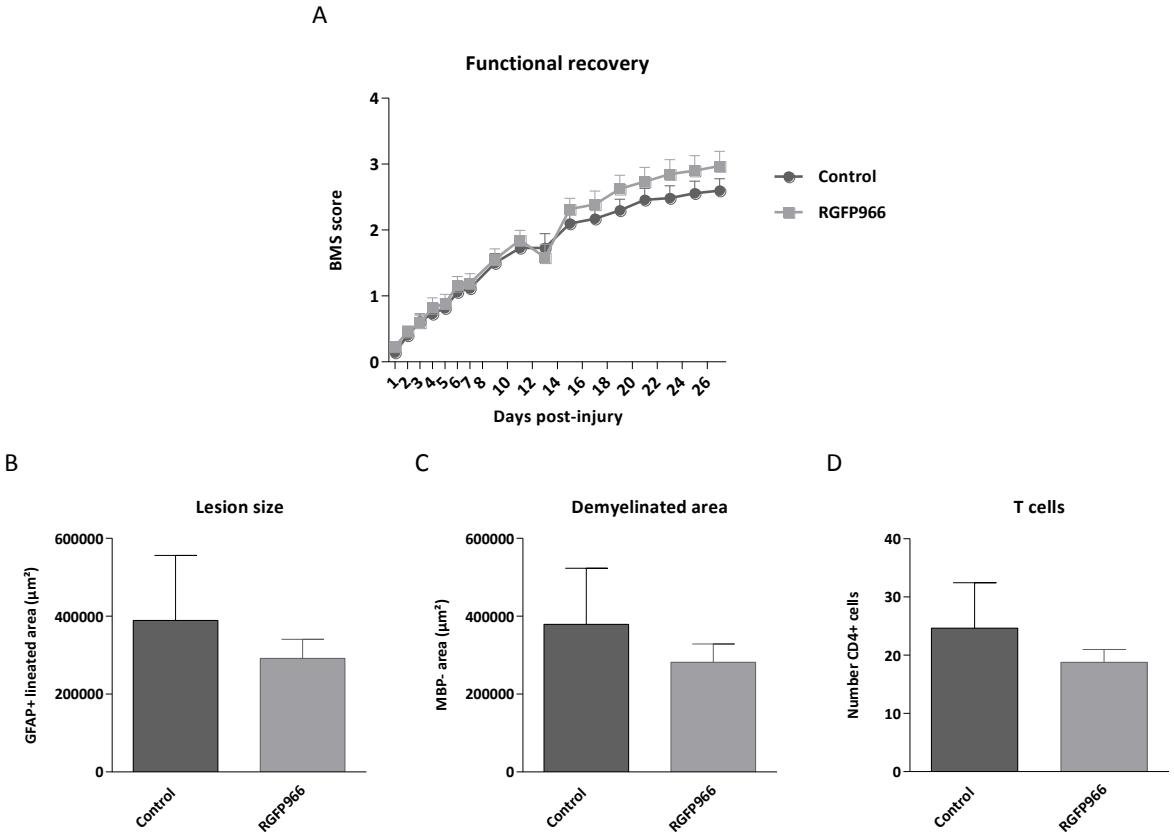

Figure 10: Four weeks after injury, treatment with RGFP966 does not change functional recovery or lesion properties. (A) Functional recovery is measured using the Basso Mouse Scale (BMS). (n=35 (control), n=36 (RGFP966), 2-way ANOVA with multiple comparison). (B) The lesion site is represented by the area lineated by GFAP-positive perilesional astrocytes. (n=6 (control), n=7 (RGFP966), student's t-test). (C) The MBP-negative area embodies demyelination of the lesion. (n=6 (control), n=7 (RGFP966), student's t-test). (D) CD4-positive cells represent the infiltrated T cells. (n=5 (control), n=5 (RGFP966), student's t-test). GFAP: glial fibrillary acidic protein; MBP: myelin basic protein; CD4: cluster of differentiation 4

3.4. RGFP966 does not modulate macrophage polarization *in vivo*

The effect of RGFP966 administration on the macrophage population *in vivo* is studied at different time points by immunohistochemical tissue analysis. Iba1 staining is used to identify the macrophages and microglia. The microglia can be distinguished from the macrophages using TMEM119. M1 and M2 macrophages are discriminated using Arg1/MHC-II double staining. Arg1-positive cells represent M2 macrophages while MHC-II-positive cells represent M1 macrophages.

Three days after the injury (3 dpi), the acute pathophysiology of SCI is represented. The microglia are already present while the macrophages are infiltrating. The presence of both cell types is unchanged by treatment of RGFP966 at rostral or caudal regions of the epicenter or at the lesion epicenter itself (Figure 11A+B). The intensity of Iba1-positive macrophages and microglia is comparable between the groups (Figure 11A), just like the TMEM119-positive microglia (Figure 11B). The number of Arg1-positive M2 macrophages does not significantly increase after treatment with RGFP966 compared to control animals (Figure 11C). Likewise, MHC-II-positive M1 macrophages do not differ in number between the groups (Figure 11D).

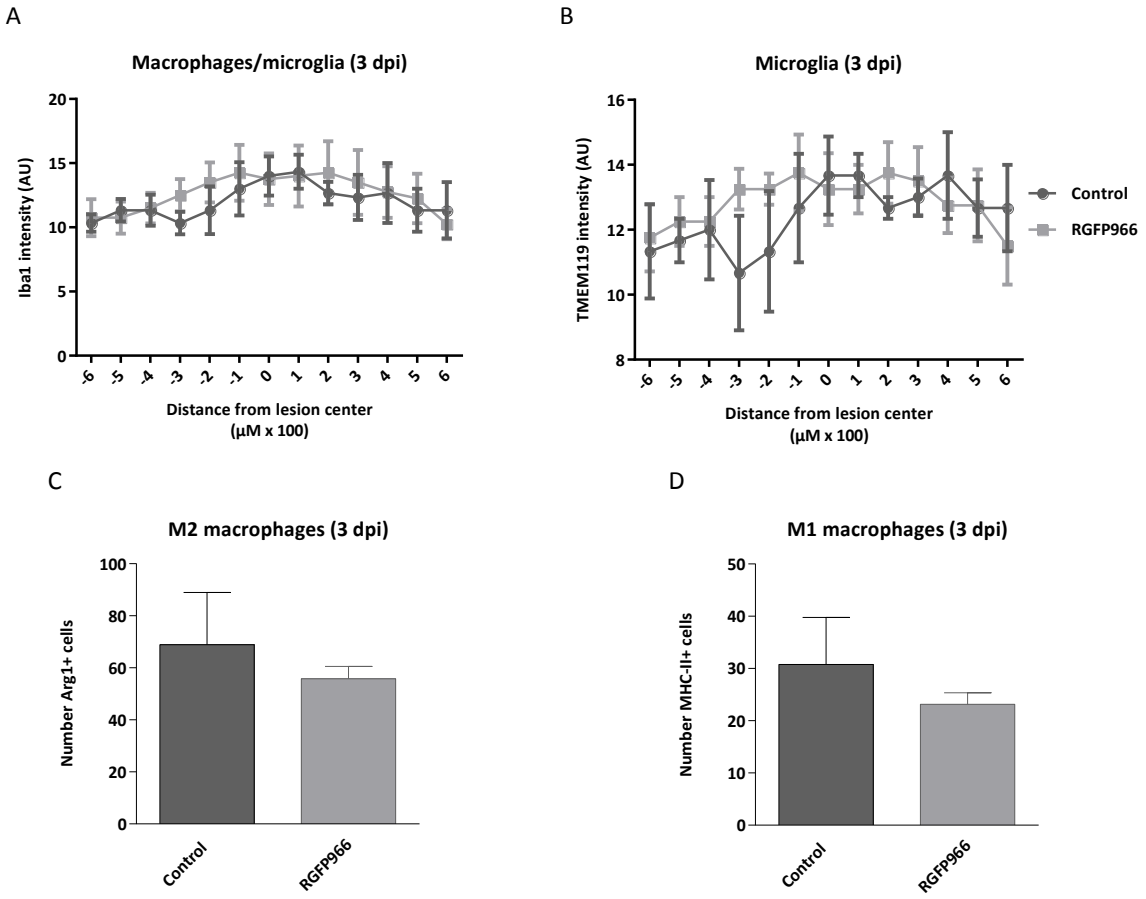

Figure 11: The presence of macrophages and microglia and their polarization is unchanged after treatment with RGFP966 three days post injury. (A) The intensity of Iba1-positive cells represents the macrophages and microglia at different sites of the lesion. (n=3 (control), n=4 (RGFP966), 2-way ANOVA with multiple comparison). (B) The intensity of TMEM119-positive cells embodies the microglia at different sites of the lesion. (n=3 (control), n=4 (RGFP966), 2-way ANOVA with multiple comparison). Analyses (A+B) were quantified within square areas of 100 x 100 mm just below the lesion site, extending 600 mm rostral to 600 mm caudal from the lesion epicenter. (C) The number of Arg1-positive cells at the lesion site represents the M2 macrophages. (n=3 (control), n=6 (RGFP966), student's t-test). (D) The number of MHC-II-positive cells at the lesion site embodies the M1 macrophages. (n=3 (control), n=6 (RGFP966), student's t-test). Iba1: ionized calcium binding adaptor molecule 1; TMEM119: transmembrane protein 119; Arg1: arginase 1; MHC-II: major histocompatibility complex class II; dpi: days post injury; AU: arbitrary unit

Next, the effect of RGFP966 on the chronic pathology, four weeks post injury (4 wpi), was evaluated. The presence of macrophages and microglia, Iba1-positive cells, does not differ between groups (Figure 12A). RGFP966 does not modulate the macrophage polarization *in vivo.* The number of Arg1-positive M2 and MHC-II-positive M1 macrophages is not affected by treatment with RGFP966 (Figure 12B+C). These results imply that RGFP966 does not control the macrophage polarization during the acute or the chronic pathology *in vivo*.

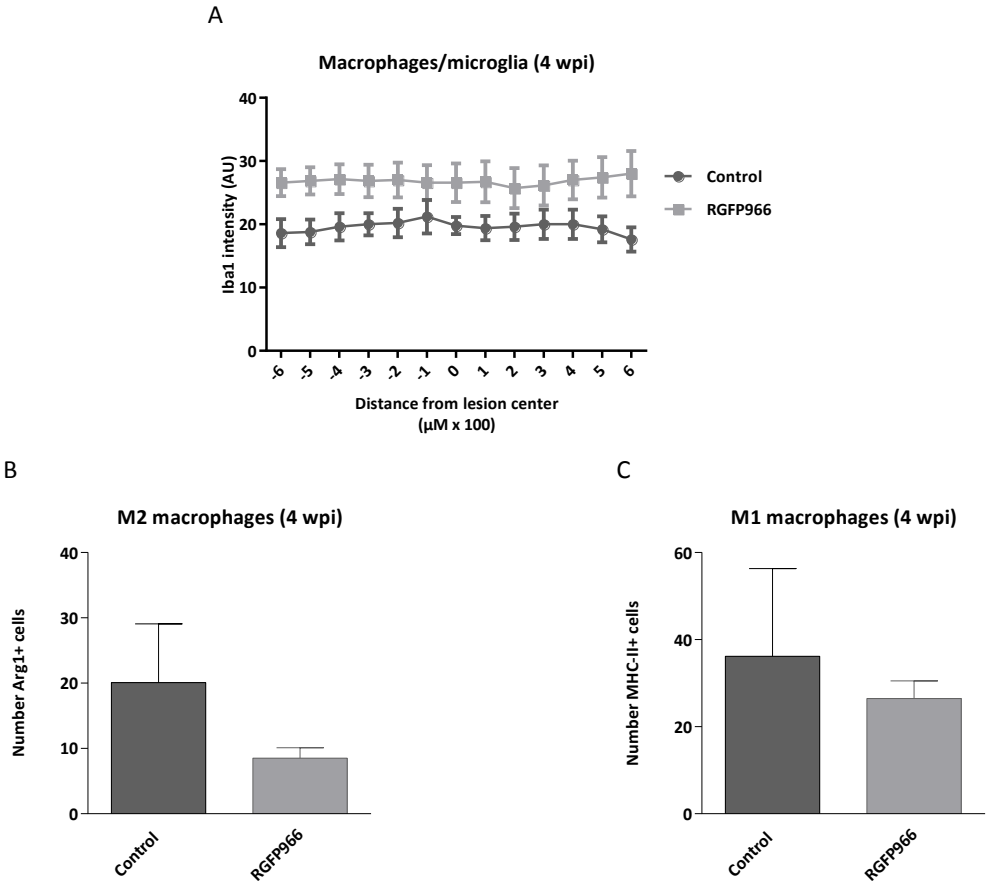

Figure 12: The presence of phagocytes neither the macrophage polarization is changed after treatment with RGFP966 four weeks after injury. (A) The intensity of Iba1-positive cells represents the macrophages and microglia at different sites of the lesion. (n=5 (control), n=7 (RGFP966), 2-way ANOVA with multiple comparison). Analyses were quantified within square areas of 100 x 100 mm just below the lesion site, extending 600 mm rostral to 600 mm caudal from the lesion epicenter. (B) The number of Arg1-positive cells at the lesion site embodies the M2 macrophages. (n=7 (control), n=6 (RGFP966), student's t-test). (C) The number of MHC-II-positive cells at the lesion site represents the M1 macrophages. (n=7 (control), n=8 (RGFP966), student's t-test). Iba-1: ionized calcium binding adaptor molecule 1; Arg1: arginase 1; MHC-II: major histocompatibility complex class II; wpi: weeks post injury; AU: arbitrary unit

4. DISCUSSION & OUTLOOK

Neuroinflammation plays a role in the pathological process of SCI. Hence, it is an important target to control in order to find an effective treatment for SCI (5, 7, 11, 19-22). Broad anti-inflammatory mediators are currently used to alleviate the symptoms and dampen secondary damage but they lack specificity, are associated with many side effects and are unable to cure the condition (2). Macrophages play an important part in the damaging neuroinflammatory response (11, 31, 32). M1 macrophages are described to block axonal regeneration, act neurotoxic and are highly present in the lesion while M2 macrophages, which are considered to be neuroprotective and promote axonal regeneration, are only transiently present (7, 19-21, 35, 37, 39, 42). Modulating the macrophage polarization has therefore been considered as an attractive option to improve outcome after SCI. This strategy has already been proven feasible in an animal model by our research group (50). HDAC3 has been identified as an epigenomic brake of the alternative M2 phenotype (59). Therefore, it is hypothesized in this study that inhibition of HDAC3, as a central regulator of macrophage polarization, will improve functional recovery in a mouse model of T-cut spinal cord hemisection injury.

To analyze the effect of the HDAC3 specific inhibitor RGFP966 on primary BMDMs, the macrophage phenotype was identified *in vitro.* Stimulation with RGFP966 enhances the gene expression of M2 markers Arg1 and Ym1a by IL-4-primed BMDMs. In addition, RGFP966 in combination with IL-4 significantly augments the protein expression of Arg1. The functionality of the enzyme, evaluated with the ability to convert L-arginine into L-ornithine and urea, tends to increase after stimulation with RGFP966. Nonetheless, this experiment needs to be repeated to verify the result. On the contrary, RGFP966 has no effect on the gene expression of selected LPS-induced M1 markers. Protein expression or functionality of these factors still needs to be analyzed to make a correct conclusion about the effect of RGFP966 on the M1 phenotype. Consequently, these results indicate that RGFP966 boosts the M2 phenotype in the presence of M2-inducing cytokine IL-4 *in vitro*. The Arg1 expression of these macrophages is increased and this suggests that RGFP966 enhances the ability of the macrophages to consume L-arginine. Literature describes that depletion of L-arginine by the persistence of Arg1-expressing M2 macrophages causes T cell anergy and thereby dampens the T cell response and associated tissue damage (38). M2 macrophages will deplete the L-arginine used by M1 macrophages as well and this competition can balance the macrophage polarization even more towards the M2 phenotype (38). To find out whether RGFP966 works through other M2-inducing cytokines as well, the experiments need to be repeated. One could use IL-13-primed macrophages in a similar *in vitro* set-up. Although both cytokines induce the M2a subdivision of the M2 phenotype and work through the same receptor component; IL-4 and IL-13 have different downstream signaling pathways (38, 64).

Phagocytosis by the macrophages is very important during SCI. Therefore, the effect of RGFP966 on the phagocytic ability of spinal cord debris by BMDMs was determined *in vitro*. It has already been shown that

persistent presence of myelin debris skews macrophage polarization towards the M1 phenotype represented by foamy macrophages (32). Results from the present study show that IL-4- and LPS-primed macrophages are able to phagocytose spinal cord debris. These macrophages become foamy after being exposed to the debris for 48 hours. Unstimulated macrophages phagocytose spinal cord debris as well to a comparable level as the IL-4- or LPS-primed macrophages. Therefore, one can assume that the spinal cord debris is the largest trigger of these cells to become activated and phagocytose the lipids. Administration of RGFP966 significantly reduces the formation of foamy macrophages, regardless of whether they are unstimulated or LPS or IL-4 primed. This result suggests that RGFP966 enables the macrophages to better handle the lipids after phagocytosis. By these means, formation of lipid-laden macrophages, which are associated with persistent inflammation and tissue damage *in vivo* (32, 38), could be reduced. The lipid homeostasis of macrophages largely depends on the expression of ABCA1 which transports the processed lipids out of the cell (65). RGFP966 could enhance the ABCA1 expression directly or indirectly via nuclear receptors PPARγ and LXR (65). Therefore, it is interesting to investigate the expression of ABCA1, PPARγ and LXR by BMDMs after stimulation with RGFP966. Especially PPARγ and LXR can give valuable insights since they are associated with immunomodulation next to their ability to directly induce transcription of ABCA1 (40, 41, 65-67). In addition, if the macrophages phagocytose and process the spinal cord debris and successfully transport lipids out of the cell, more free cholesterol is available for remyelination (32). On the other hand, it is possible that the macrophages no longer phagocytose the spinal cord debris after stimulation with RGFP966. Macrophages take up tissue debris through scavenger receptors and endocytosis (68). RGFP966 could interfere with these processes leading to a decrease in phagocytic ability. Again, looking at the expression levels of these receptors after stimulation with RGFP966 could give more insight into the effect of the inhibitor on the phagocytic ability of the macrophages.

Preliminary data indicates that RGFP966 significantly increases the acetylation levels of histone 3. Nevertheless, it is possible that the described *in vitro* results are not achieved by histone modification; HDACs can affect other proteins as well. The PPARγ receptor can be regulated by posttranslational modifications and HDAC3 has found to have a direct effect on the PPARγ protein in mature adipocytes (69). Inhibition of HDAC3, resulting in acetylation of PPARγ, induces the transcription of PPARγ target genes without interaction of a ligand (69). It is possible that the same happens in macrophages as well. To investigate this, the acetylation level of PPARγ protein could be studied. Consequently, HDAC3 could control the M2 phenotype via direct, ligand-independent activation of PPARγ and transcription of its anti-inflammatory target genes or as the previously described epigenomic brake.

In this study we show that RGFP966 stimulates the M2 polarization *in vitro* at the cellular level. However, *in vivo* in the mouse model of SCI, RGFP966 does not affect functional recovery nor does it affect the histopathological processes. Using the Basso Mouse Scale, no functional improvements are detected after treatment with RGFP966. To investigate what happened on histological level, immunohistochemical analyses have been performed on representative cryosections of the spinal cords. Both the lesion size and demyelinated

area, important characteristics of the lesion and associated damage, are similar in the treatment and control group. The infiltration of immune cells does not differ after treatment with RGFP966. The number of infiltrated T cells, represented by the CD4-positive cells, is the same in both groups. The presence of phagocytic cells, including macrophages and microglia, does not differ at rostral or caudal regions of the epicenter or at the lesion epicenter itself after treatment with RGFP966 during the acute (3 dpi) or chronic (4 wpi) pathology of SCI. Moreover, the macrophage polarization is not altered under influence of RGFP966, neither when macrophages are infiltrating at 3 dpi nor during the chronic phase when they are already present in the lesion. Both the Arg1-positive M2 and MHC-II-positive M1 macrophages are unaffected by the HDAC3 inhibitor *in vivo*.

From the *in vitro* results and literature, it was expected that RGFP966 would improve functional recovery in the mouse model of SCI by modulating the macrophage polarization. However, no improvement has been observed in this study *in vivo.* An explanation for this is that the potential effect of RGFP966 might be overruled by the complexity of the pathophysiology of SCI. Especially pro-inflammatory cytokines are present in the lesion (19, 46). RGFP966, however, seems to be unable to decrease the gene expression of pro-inflammatory M1 markers by LPS-primed BMDMs in our *in vitro* results whereas the IL-4-induced M2 phenotype is boosted. Therefore, it is plausible that the beneficial effects of RGFP966 on the M2 polarization only occur in the presence of M2-inducing cytokines. However, the presence of M2-inducing cytokines IL-4, IL-13 and IL-10 is very low in the lesion environment during SCI (19). In addition, RGFP966 reduces the formation of foamy macrophages *in vitro.* However, it is not yet known whether this is caused by an increase in the lipid homeostasis or a decrease in the phagocytic ability of these macrophages. When less tissue debris is phagocytosed by the macrophages, the debris could persist in the lesion and block axonal regeneration to a higher extend. Another explanation is the administration route. In the current experimental set-up, RGFP966 was intraperitoneally administered. It is possible that the inhibitor does not reach the lesion or the concentration is too low to elicit a biological relevant effect. To test this, the potency of the inhibitor needs to be determined by looking at the acetylation levels of histones of the spinal cord. Besides, intravenous or intralesional injections could be alternative options but are more difficult to perform in mice. To sidestep the problems of the administration route and the potential of an inhibitor, the genetic knockout of HDAC3 in the myeloid cells ($HDAC3^{flox/flox}$;LysMCre) could be used (60). Repeating the experiments in this model would be interesting to further elucidate the potential effects of HDAC3 in SCI in a more specific way. Unfortunately, this model has its own setbacks since the knockout is not specifically in macrophages but in all myeloid cells including neutrophils. Furthermore, female mice were used in this experiment and they have an advantage during SCI: activation of G-protein coupled estrogen receptor 1 is described to be neuroprotective (70). It is possible that the effect of RGFP966 is undetectable due to the initial smaller lesions causing a limited effect size. To rule this factor out, the *in vivo* experiments should be repeated using males.

In this study, we focus on the neuroinflammatory reaction. The immune response starts within the first day after the injury. As previously described, the macrophages play an important role in the detrimental

inflammatory process (5, 7, 11, 19-22). In the present set-up, the macrophages were histologically analyzed during infiltration (3 dpi) or during the chronic phase. However, looking at a time point in between, for example during the subacute phase lasting up to two weeks, could be valuable since the immune response is at point and actively affecting the tissue. Before macrophages infiltrate, neutrophils are already present in the lesion starting from the first day. It is possible that RGFP966 influences these cells as well since it is administrated two hours after the surgery. It has been described that global HDAC inhibitors induce apoptosis of humane neutrophils (71). It is possible that inhibition of HDAC3 affects the neutrophils in the used mouse model in the same way. Therefore, one could look at the neutrophil infiltration three days post injury. It is known that macrophages eliminate apoptotic neutrophils, thereby preventing the toxic contents of neutrophils to leak into the lesion which would otherwise cause an exaggerated and persistent inflammatory response (32). However, when the apoptotic neutrophils precede and overwhelm the macrophage response, this could counteract the beneficial effect of RGFP966 on the macrophages explaining why no improved functionality has been observed. As seen in SCI, HDAC3 expression is elevated in the PBMCs of patients suffering from multiple sclerosis (MS) (57, 72). It has been shown that these autoreactive lymphocytes are resistant to induced apoptosis (72). Inhibition of HDAC3 could control the inflammatory response of lymphocytes in the used mouse model of SCI as well. However, there is no effect of RGFP966 on the CD4-positive T cell infiltration *in vivo*.

HDAC3 has already been suggested to control the macrophage polarization and this finding has been strengthened by our own *in vitro* results. However, RGFP966 has no effect *in vivo* in this study. It does not improve the recovery after SCI and does not modulate the macrophage polarization *in vivo*. These results raise the question whether RGFP966 is potent and reaches the lesion and whether HDAC3 is the specific HDAC isoform that is involved in the process affecting the functional recovery, as shown by previous studies using a wide HDAC inhibitor (52, 53, 56). Other HDAC isoforms are involved in the inflammatory response of macrophages as well. Research has found that HDAC5 and HDAC7 promote the LPS-induced inflammatory response (73, 74). HDAC11 is described to suppress the LPS-induced expression of IL-10 (75). Therefore, targeting these HDACs could be an alternative to HDAC3, however, more research is needed.

The hypothesis of the study is not yet confirmed nor rejected. The proposed adaptations and future experiments could further elucidate the effect of HDAC3 on the macrophage polarization and thereby on the functional recovery.

5. CONCLUSION

This study aimed to elucidate the effect of HDAC3 on the macrophage polarization in the context of functional recovery after SCI. Therefore, it was hypothesized that inhibition of HDAC3, as a central regulator of macrophage polarization, would improve functional recovery in a mouse model of T-cut spinal cord hemisection injury. First, the macrophage phenotype and phagocytic capacity of M1- or M2-primed BMDMs after stimulation with RGFP966 was evaluated *in vitro*. Results show that RGFP966 boosts the IL-4-induced M2 phenotype characterized by Arg1 expression. These data are promising for the *in vivo* experiments since the M2 macrophages are correlated with axonal regeneration, neuroprotection and immunomodulation. In contrast, RGFP966 has no effect on the LPS-induced gene expression of selected M1-associated markers *in vitro*. In addition, RGFP966 reduces the formation of foamy, lipid-laden macrophages in the presence of spinal cord debris *in vitro*, regardless of their state of activation. However, it needs to be further unraveled whether RGFP966 enables these macrophages to maintain their lipid homeostasis or whether it reduces the phagocytic ability of the macrophages.

Unfortunately, RGFP966 does not improve functional recovery in a mouse model of T-cut spinal cord hemisection injury. Evaluation of the spinal cords reveals that neither the phagocytic population nor their polarization is changed by treatment with RGFP966 on acute or long term *in vivo*. Since RGFP966 is unable to affect expression of inflammatory genes associated with M1 phenotype *in vitro,* it is likely that, if the inhibitor reaches the lesion in appropriate concentrations, it cannot decrease the M1 polarization *in vivo*. Likewise, *in vitro* data indicates that RGFP966 can boost the IL-4-induced phenotype but low amounts of M2-promoting cytokines are present in the lesion during SCI. Therefore, the potential effect of RGFP966 could get lost in the complicated pathology of SCI and thus could not be strong enough to induce a functional recovery *in vivo*.

In conclusion, the achieved results in this study cannot confirm the stated hypothesis, however, it cannot yet be rejected either because of the promising *in vitro* results on the macrophage polarization. Therefore, further research is needed and especially repeating the *in vivo* experiments using myeloid cell-specific HDAC3 knockout mice could give valuable insight in the role of HDAC3 on the macrophage polarization and thereby on the functional recovery.

REFERENCES

1. Afshari FT, Kappagantula S, Fawcett JW. Extrinsic and intrinsic factors controlling axonal regeneration after spinal cord injury. Expert reviews in molecular medicine. 2009;11:e37.
2. Rowland JW, Hawryluk GW, Kwon B, Fehlings MG. Current status of acute spinal cord injury pathophysiology and emerging therapies: promise on the horizon. Neurosurg Focus. 2008;25(5):E2.
3. Sezer N, Akkus S, Ugurlu FG. Chronic complications of spinal cord injury. World J Orthop. 2015;6(1):24-33.
4. Kwon BK, Tetzlaff W, Grauer JN, Beiner J, Vaccaro AR. Pathophysiology and pharmacologic treatment of acute spinal cord injury. Spine J. 2004;4(4):451-64.
5. Wong JK, Zou H. Reshaping the chromatin landscape after spinal cord injury. Frontiers in biology. 2014;9(5):356-66.
6. Evans TA, Barkauskas DS, Myers JT, Hare EG, You JQ, Ransohoff RM, et al. High-resolution intravital imaging reveals that blood-derived macrophages but not resident microglia facilitate secondary axonal dieback in traumatic spinal cord injury. Experimental neurology. 2014;254:109-20.
7. Horn KP, Busch SA, Hawthorne AL, van Rooijen N, Silver J. Another barrier to regeneration in the CNS: activated macrophages induce extensive retraction of dystrophic axons through direct physical interactions. The Journal of neuroscience : the official journal of the Society for Neuroscience. 2008;28(38):9330-41.
8. Kerschensteiner M, Schwab ME, Lichtman JW, Misgeld T. In vivo imaging of axonal degeneration and regeneration in the injured spinal cord. Nature medicine. 2005;11(5):572-7.
9. Hill CE. A view from the ending: Axonal dieback and regeneration following SCI. Neuroscience letters. 2016.
10. Raff MC, Whitmore AV, Finn JT. Axonal self-destruction and neurodegeneration. Science. 2002;296(5569):868-71.
11. Alexander JK, Popovich PG. Neuroinflammation in spinal cord injury: therapeutic targets for neuroprotection and regeneration. Progress in brain research. 2009;175:125-37.
12. Silver J, Miller JH. Regeneration beyond the glial scar. Nature reviews Neuroscience. 2004;5(2):146-56.
13. Fawcett JW, Asher RA. The glial scar and central nervous system repair. Brain research bulletin. 1999;49(6):377-91.
14. Faulkner JR, Herrmann JE, Woo MJ, Tansey KE, Doan NB, Sofroniew MV. Reactive astrocytes protect tissue and preserve function after spinal cord injury. The Journal of neuroscience : the official journal of the Society for Neuroscience. 2004;24(9):2143-55.
15. Windle WF, Clemente CD, Chambers WW. Inhibition of formation of a glial barrier as a means of permitting a peripheral nerve to grow into the brain. The Journal of comparative neurology. 1952;96(2):359-69.
16. Kwok JC, Afshari F, Garcia-Alias G, Fawcett JW. Proteoglycans in the central nervous system: plasticity, regeneration and their stimulation with chondroitinase ABC. Restorative neurology and neuroscience. 2008;26(2-3):131-45.
17. Niclou SP, Ehlert EM, Verhaagen J. Chemorepellent axon guidance molecules in spinal cord injury. Journal of neurotrauma. 2006;23(3-4):409-21.
18. Filbin MT. Myelin-associated inhibitors of axonal regeneration in the adult mammalian CNS. Nature reviews Neuroscience. 2003;4(9):703-13.
19. Kigerl KA, Gensel JC, Ankeny DP, Alexander JK, Donnelly DJ, Popovich PG. Identification of two distinct macrophage subsets with divergent effects causing either neurotoxicity or regeneration in the injured mouse spinal cord. The Journal of neuroscience : the official journal of the Society for Neuroscience. 2009;29(43):13435-44.
20. Donnelly DJ, Popovich PG. Inflammation and its role in neuroprotection, axonal regeneration and functional recovery after spinal cord injury. Experimental neurology. 2008;209(2):378-88.
21. McPhail LT, Stirling DP, Tetzlaff W, Kwiecien JM, Ramer MS. The contribution of activated phagocytes and myelin degeneration to axonal retraction/dieback following spinal cord injury. The European journal of neuroscience. 2004;20(8):1984-94.
22. Giulian D, Robertson C. Inhibition of mononuclear phagocytes reduces ischemic injury in the spinal cord. Annals of neurology. 1990;27(1):33-42.

23. Mothe AJ, Tator CH. Advances in stem cell therapy for spinal cord injury. The Journal of clinical investigation. 2012;122(11):3824-34.
24. Peruzzotti-Jametti L, Donega M, Giusto E, Mallucci G, Marchetti B, Pluchino S. The role of the immune system in central nervous system plasticity after acute injury. Neuroscience. 2014;283:210-21.
25. Yang L, Blumbergs PC, Jones NR, Manavis J, Sarvestani GT, Ghabriel MN. Early expression and cellular localization of proinflammatory cytokines interleukin-1beta, interleukin-6, and tumor necrosis factor-alpha in human traumatic spinal cord injury. Spine. 2004;29(9):966-71.
26. Weber C, Fraemohs L, Dejana E. The role of junctional adhesion molecules in vascular inflammation. Nature reviews Immunology. 2007;7(6):467-77.
27. Engelhardt B, Ransohoff RM. The ins and outs of T-lymphocyte trafficking to the CNS: anatomical sites and molecular mechanisms. Trends in immunology. 2005;26(9):485-95.
28. Fleming JC, Norenberg MD, Ramsay DA, Dekaban GA, Marcillo AE, Saenz AD, et al. The cellular inflammatory response in human spinal cords after injury. Brain : a journal of neurology. 2006;129(Pt 12):3249-69.
29. Taoka Y, Okajima K, Uchiba M, Murakami K, Kushimoto S, Johno M, et al. Role of neutrophils in spinal cord injury in the rat. Neuroscience. 1997;79(4):1177-82.
30. Neirinckx V, Coste C, Franzen R, Gothot A, Rogister B, Wislet S. Neutrophil contribution to spinal cord injury and repair. J Neuroinflammation. 2014;11:150.
31. Chang HT. Subacute human spinal cord contusion: few lymphocytes and many macrophages. Spinal cord. 2007;45(2):174-82.
32. Wang X, Cao K, Sun X, Chen Y, Duan Z, Sun L, et al. Macrophages in spinal cord injury: phenotypic and functional change from exposure to myelin debris. Glia. 2015;63(4):635-51.
33. Hines DJ, Hines RM, Mulligan SJ, Macvicar BA. Microglia processes block the spread of damage in the brain and require functional chloride channels. Glia. 2009;57(15):1610-8.
34. Mantovani A, Sica A, Sozzani S, Allavena P, Vecchi A, Locati M. The chemokine system in diverse forms of macrophage activation and polarization. Trends in immunology. 2004;25(12):677-86.
35. Hu X, Leak RK, Shi Y, Suenaga J, Gao Y, Zheng P, et al. Microglial and macrophage polarization-new prospects for brain repair. Nat Rev Neurol. 2015;11(1):56-64.
36. Busch SA, Horn KP, Silver DJ, Silver J. Overcoming macrophage-mediated axonal dieback following CNS injury. The Journal of neuroscience : the official journal of the Society for Neuroscience. 2009;29(32):9967-76.
37. Goerdt S, Orfanos CE. Other functions, other genes: alternative activation of antigen-presenting cells. Immunity. 1999;10(2):137-42.
38. Roszer T. Understanding the Mysterious M2 Macrophage through Activation Markers and Effector Mechanisms. Mediators Inflamm. 2015;2015:816460.
39. Wang G, Shi Y, Jiang X, Leak RK, Hu X, Wu Y, et al. HDAC inhibition prevents white matter injury by modulating microglia/macrophage polarization through the GSK3beta/PTEN/Akt axis. Proceedings of the National Academy of Sciences of the United States of America. 2015;112(9):2853-8.
40. Odegaard JI, Ricardo-Gonzalez RR, Goforth MH, Morel CR, Subramanian V, Mukundan L, et al. Macrophage-specific PPARgamma controls alternative activation and improves insulin resistance. Nature. 2007;447(7148):1116-20.
41. Bogie JF, Timmermans S, Huynh-Thu VA, Irrthum A, Smeets HJ, Gustafsson JA, et al. Myelin-derived lipids modulate macrophage activity by liver X receptor activation. PloS one. 2012;7(9):e44998.
42. Bethea JR, Nagashima H, Acosta MC, Briceno C, Gomez F, Marcillo AE, et al. Systemically administered interleukin-10 reduces tumor necrosis factor-alpha production and significantly improves functional recovery following traumatic spinal cord injury in rats. Journal of neurotrauma. 1999;16(10):851-63.
43. Miron VE, Boyd A, Zhao JW, Yuen TJ, Ruckh JM, Shadrach JL, et al. M2 microglia and macrophages drive oligodendrocyte differentiation during CNS remyelination. Nature neuroscience. 2013;16(9):1211-8.
44. Stout RD, Jiang C, Matta B, Tietzel I, Watkins SK, Suttles J. Macrophages sequentially change their functional phenotype in response to changes in microenvironmental influences. Journal of immunology. 2005;175(1):342-9.
45. David S, Kroner A. Repertoire of microglial and macrophage responses after spinal cord injury. Nature reviews Neuroscience. 2011;12(7):388-99.
46. Yakovlev AG, Faden AI. Sequential expression of c-fos protooncogene, TNF-alpha, and dynorphin genes in spinal cord following experimental traumatic injury. Molecular and chemical neuropathology / sponsored by

the International Society for Neurochemistry and the World Federation of Neurology and research groups on neurochemistry and cerebrospinal fluid. 1994;23(2-3):179-90.
47. Zhou X, He X, Ren Y. Function of microglia and macrophages in secondary damage after spinal cord injury. Neural Regen Res. 2014;9(20):1787-95.
48. Oudega M, Vargas CG, Weber AB, Kleitman N, Bunge MB. Long-term effects of methylprednisolone following transection of adult rat spinal cord. The European journal of neuroscience. 1999;11(7):2453-64.
49. Mosser DM, Edwards JP. Exploring the full spectrum of macrophage activation. Nature reviews Immunology. 2008;8(12):958-69.
50. Dooley D, Lemmens E, Vangansewinkel T, Le Blon D, Hoornaert C, Ponsaerts P, et al. Cell-Based Delivery of Interleukin-13 Directs Alternative Activation of Macrophages Resulting in Improved Functional Outcome after Spinal Cord Injury. Stem Cell Reports. 2016;7(6):1099-115.
51. Kouzarides T. Chromatin modifications and their function. Cell. 2007;128(4):693-705.
52. Lv L, Sun Y, Han X, Xu CC, Tang YP, Dong Q. Valproic acid improves outcome after rodent spinal cord injury: potential roles of histone deacetylase inhibition. Brain Res. 2011;1396:60-8.
53. Lv L, Han X, Sun Y, Wang X, Dong Q. Valproic acid improves locomotion in vivo after SCI and axonal growth of neurons in vitro. Experimental neurology. 2012;233(2):783-90.
54. Mottamal M, Zheng S, Huang TL, Wang G. Histone deacetylase inhibitors in clinical studies as templates for new anticancer agents. Molecules. 2015;20(3):3898-941.
55. McCann KE, Rosenhauer AM, Jones GM, Norvelle A, Choi DC, Huhman KL. Histone deacetylase and acetyltransferase inhibitors modulate behavioral responses to social stress. Psychoneuroendocrinology. 2016;75:100-9.
56. Lee JY, Kim HS, Choi HY, Oh TH, Ju BG, Yune TY. Valproic acid attenuates blood-spinal cord barrier disruption by inhibiting matrix metalloprotease-9 activity and improves functional recovery after spinal cord injury. Journal of neurochemistry. 2012;121(5):818-29.
57. Ma YD, Fang J, Liu H, Zhou L. Increased HDAC3 and decreased miRNA-130a expression in PBMCs through recruitment HDAC3 in patients with spinal cord injuries. Int J Clin Exp Pathol. 2015;8(2):1682-9.
58. Chen X, Barozzi I, Termanini A, Prosperini E, Recchiuti A, Dalli J, et al. Requirement for the histone deacetylase Hdac3 for the inflammatory gene expression program in macrophages. Proceedings of the National Academy of Sciences of the United States of America. 2012;109(42):E2865-74.
59. Mullican SE, Gaddis CA, Alenghat T, Nair MG, Giacomin PR, Everett LJ, et al. Histone deacetylase 3 is an epigenomic brake in macrophage alternative activation. Genes & development. 2011;25(23):2480-8.
60. Hoeksema MA, Gijbels MJ, Van den Bossche J, van der Velden S, Sijm A, Neele AE, et al. Targeting macrophage Histone deacetylase 3 stabilizes atherosclerotic lesions. EMBO Mol Med. 2014;6(9):1124-32.
61. Boato F, Hendrix S, Huelsenbeck SC, Hofmann F, Grosse G, Djalali S, et al. C3 peptide enhances recovery from spinal cord injury by improved regenerative growth of descending fiber tracts. J Cell Sci. 2010;123(Pt 10):1652-62.
62. Walsh JT, Hendrix S, Boato F, Smirnov I, Zheng J, Lukens JR, et al. MHCII-independent CD4+ T cells protect injured CNS neurons via IL-4. The Journal of clinical investigation. 2015;125(6):2547.
63. Basso DM, Fisher LC, Anderson AJ, Jakeman LB, McTigue DM, Popovich PG. Basso Mouse Scale for locomotion detects differences in recovery after spinal cord injury in five common mouse strains. Journal of neurotrauma. 2006;23(5):635-59.
64. Bhattacharjee A, Shukla M, Yakubenko VP, Mulya A, Kundu S, Cathcart MK. IL-4 and IL-13 employ discrete signaling pathways for target gene expression in alternatively activated monocytes/macrophages. Free Radic Biol Med. 2013;54:1-16.
65. Chawla A, Boisvert WA, Lee CH, Laffitte BA, Barak Y, Joseph SB, et al. A PPAR gamma-LXR-ABCA1 pathway in macrophages is involved in cholesterol efflux and atherogenesis. Molecular cell. 2001;7(1):161-71.
66. Orasanu G, Ziouzenkova O, Devchand PR, Nehra V, Hamdy O, Horton ES, et al. The peroxisome proliferator-activated receptor-gamma agonist pioglitazone represses inflammation in a peroxisome proliferator-activated receptor-alpha-dependent manner in vitro and in vivo in mice. J Am Coll Cardiol. 2008;52(10):869-81.
67. Bensinger SJ, Tontonoz P. Integration of metabolism and inflammation by lipid-activated nuclear receptors. Nature. 2008;454(7203):470-7.
68. Aderem A, Underhill DM. Mechanisms of phagocytosis in macrophages. Annual review of immunology. 1999;17:593-623.

69. Jiang X, Ye X, Guo W, Lu H, Gao Z. Inhibition of HDAC3 promotes ligand-independent PPARgamma activation by protein acetylation. J Mol Endocrinol. 2014;53(2):191-200.
70. Hu R, Sun H, Zhang Q, Chen J, Wu N, Meng H, et al. G-protein coupled estrogen receptor 1 mediated estrogenic neuroprotection against spinal cord injury. Crit Care Med. 2012;40(12):3230-7.
71. Kankaanranta H, Janka-Junttila M, Ilmarinen-Salo P, Ito K, Jalonen U, Ito M, et al. Histone deacetylase inhibitors induce apoptosis in human eosinophils and neutrophils. J Inflamm (Lond). 2010;7:9.
72. Zhang F, Shi Y, Wang L, Sriram S. Role of HDAC3 on p53 expression and apoptosis in T cells of patients with multiple sclerosis. PloS one. 2011;6(2):e16795.
73. Poralla L, Stroh T, Erben U, Sittig M, Liebig S, Siegmund B, et al. Histone deacetylase 5 regulates the inflammatory response of macrophages. J Cell Mol Med. 2015;19(9):2162-71.
74. Shakespear MR, Hohenhaus DM, Kelly GM, Kamal NA, Gupta P, Labzin LI, et al. Histone deacetylase 7 promotes Toll-like receptor 4-dependent proinflammatory gene expression in macrophages. The Journal of biological chemistry. 2013;288(35):25362-74.
75. Villagra A, Cheng F, Wang HW, Suarez I, Glozak M, Maurin M, et al. The histone deacetylase HDAC11 regulates the expression of interleukin 10 and immune tolerance. Nature immunology. 2009;10(1):92-100.

SUPPLEMENTS

Supplementary tables

Supplementary Table 1: The sequences of the primers used for qPCR.

Gene	Forward primer	Reverse primer
Arg1	GTGAAGAACCCACGGTCTGT	GCCAGAGATGCTTCCAACTG
CD38	ACTGGAGAGCCTACCACGAA	TGGGCCAGGTGTTTGGATTT
FIZZ	TCCAGCTAACTATCCCTCCACTGT	GGCCCATCTGTTCATAGTCTTGA
FPR2	TCTACCATCTCCAGAGTTCTGTGG	TTACATCTACCACAATGTGAACTA
GPR18	CAGACAGGAGGTTCTACATACCA	AGCGAGGCTTGGGTAAAACA
HMBS	GATGGGCAACTGTACCTGACTG	CTGGGCTCCTCTTGGAATG
IL-1β	ACCCTGCAGCTGGAGAGTGT	TTGACTTCTATCTTGTTGAAGACAAACC
IL-6	TGTCTATACCACTTCACAAGTCGGAG	GCACAACTCTTTTCTCATTTCCAC
iNOS	GGCAGCCTGTGAGACCTTTG	GCATTGGAAGTGAAGCGTTTC
Ym1a	GGGCATACCTTTATCCTGAG	CCACTGAAGTCATCCATGTC
YWHAZ	GCAACGATGTACTGTCTCTTTTGG	GTCCACAATTCCTTTCTTGTCATC

Supplementary figures

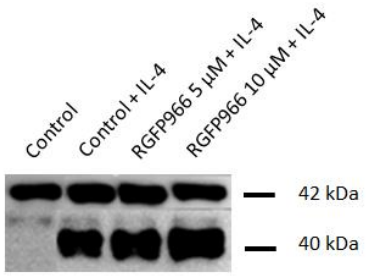

Supplementary Figure 1: The protein expression of Arg1 by IL-4-primed macrophages is enhanced by RGFP966. BMDMs were primed with IL-4 before stimulation with RGFP966. Proteins were isolated and analyzed using western blot for β-actin (42 kDa) and Arg1 (40 kDa) expression. Graph is represented in Figure 8. IL-4: interleukin-4, Arg1: arginase 1

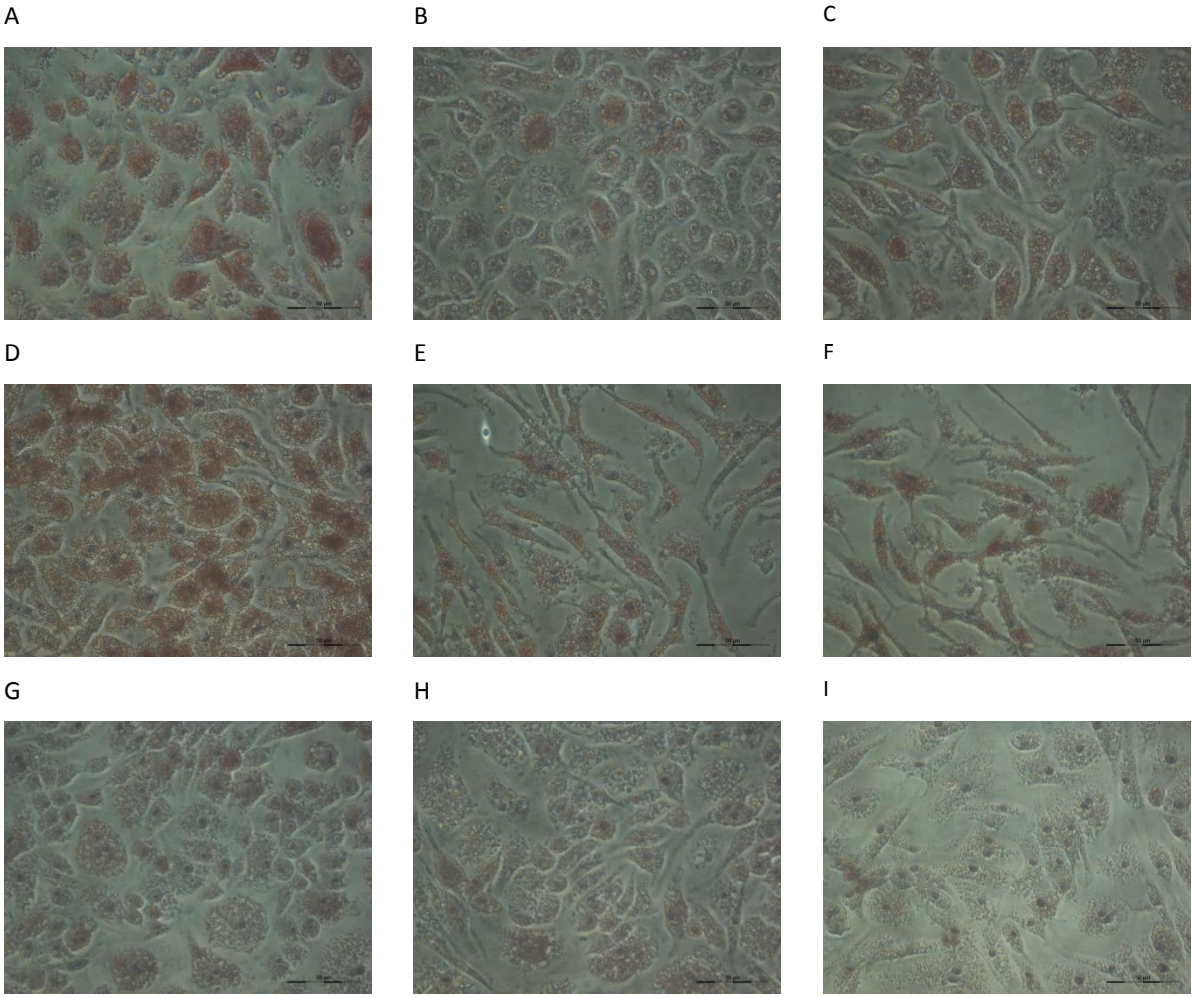

Supplementary Figure 2: RGFP966 reduces the formation of naïve, LPS- and IL-4-primed BMDMs into foamy macrophages in the presence of spinal cord debris for 48 hours *in vitro*. (A-C) Microscopy image of the Oil Red O staining after treatment with IL-4 (A) combined with 5 µM (B) or 10 µM (C) RGFP966 in the presence of spinal cord debris. (D-F) Microscopy image of the Oil Red O staining after treatment with LPS (D) combined with 5 µM (E) or 10 µM (F) RGFP966 in the presence of spinal cord debris. (G-I) Microscopy image of the Oil Red O staining in the presence of spinal cord debris alone (G) or combined with 5 µM (H) or 10 µM (I) RGFP966. Intracellular lipids are stained in red and nuclei in purple. Graph is represented in Figure 9. Scale bar: 50 µm. IL-4: interleukin-4, LPS: lipopolysaccharide

Auteursrechtelijke overeenkomst

Ik/wij verlenen het wereldwijde auteursrecht voor de ingediende eindverhandeling:
The use of a specific HDAC3 inhibitor to modulate macrophage polarization in order to improve functional recovery after spinal cord injury

Richting: **Master of Biomedical Sciences-Clinical Molecular Sciences**
Jaar: **2017**

in alle mogelijke mediaformaten, - bestaande en in de toekomst te ontwikkelen - , aan de Universiteit Hasselt.

Niet tegenstaand deze toekenning van het auteursrecht aan de Universiteit Hasselt behoud ik als auteur het recht om de eindverhandeling, - in zijn geheel of gedeeltelijk -, vrij te reproduceren, (her)publiceren of distribueren zonder de toelating te moeten verkrijgen van de Universiteit Hasselt.

Ik bevestig dat de eindverhandeling mijn origineel werk is, en dat ik het recht heb om de rechten te verlenen die in deze overeenkomst worden beschreven. Ik verklaar tevens dat de eindverhandeling, naar mijn weten, het auteursrecht van anderen niet overtreedt.

Ik verklaar tevens dat ik voor het materiaal in de eindverhandeling dat beschermd wordt door het auteursrecht, de nodige toelatingen heb verkregen zodat ik deze ook aan de Universiteit Hasselt kan overdragen en dat dit duidelijk in de tekst en inhoud van de eindverhandeling werd genotificeerd.

Universiteit Hasselt zal mij als auteur(s) van de eindverhandeling identificeren en zal geen wijzigingen aanbrengen aan de eindverhandeling, uitgezonderd deze toegelaten door deze overeenkomst.

Voor akkoord,

Baeten, Paulien

Datum: **8/06/2017**